ESCUELA TÉCNICA SUPERIOR DE INGENIERÍA (ICAI)

MÁSTER EN INGENIERÍA INDUSTRIAL

CRUISE-SHIP ENERGY SYSTEM DESIGN AND OPTIMIZATION UNDER UNCERTAINTY

Autor: Nuria Cobo-Losey Rodríguez
Director: Francois Maréchal
Supervisores: Stefano Moret y Francesco Baldi

Madrid
Agosto 2018

AUTORIZACIÓN PARA LA DIGITALIZACIÓN, DEPÓSITO Y DIVULGACIÓN EN RED DE PROYECTOS FIN DE GRADO, FIN DE MÁSTER, TESINAS O MEMORIAS DE BACHILLERATO

1º. Declaración de la autoría y acreditación de la misma.

El autor Dña. ____NURIA COBO-LOSEY RODRÍGUEZ_____

DECLARA ser el titular de los derechos de propiedad intelectual de la obra:

CRUISE-SHIP ENERGY SYSTEM DESIGN AND OPTIMIZATION UNDER UNCERTAINTY,

que ésta es una obra original, y que ostenta la condición de autor en el sentido que otorga la Ley de Propiedad Intelectual.

2º. Objeto y fines de la cesión.

Con el fin de dar la máxima difusión a la obra citada a través del Repositorio institucional de la Universidad, el autor **CEDE** a la Universidad Pontificia Comillas, de forma gratuita y no exclusiva, por el máximo plazo legal y con ámbito universal, los derechos de digitalización, de archivo, de reproducción, de distribución y de comunicación pública, incluido el derecho de puesta a disposición electrónica, tal y como se describen en la Ley de Propiedad Intelectual. El derecho de transformación se cede a los únicos efectos de lo dispuesto en la letra a) del apartado siguiente.

3º. Condiciones de la cesión y acceso

Sin perjuicio de la titularidad de la obra, que sigue correspondiendo a su autor, la cesión de derechos contemplada en esta licencia habilita para:

a) Transformarla con el fin de adaptarla a cualquier tecnología que permita incorporarla a internet y hacerla accesible; incorporar metadatos para realizar el registro de la obra e incorporar "marcas de agua" o cualquier otro sistema de seguridad o de protección.
b) Reproducirla en un soporte digital para su incorporación a una base de datos electrónica, incluyendo el derecho de reproducir y almacenar la obra en servidores, a los efectos de garantizar su seguridad, conservación y preservar el formato.
c) Comunicarla, por defecto, a través de un archivo institucional abierto, accesible de modo libre y gratuito a través de internet.
d) Cualquier otra forma de acceso (restringido, embargado, cerrado) deberá solicitarse expresamente y obedecer a causas justificadas.
e) Asignar por defecto a estos trabajos una licencia Creative Commons.
f) Asignar por defecto a estos trabajos un HANDLE (URL *persistente).*

4º. Derechos del autor.

El autor, en tanto que titular de una obra tiene derecho a:

a) Que la Universidad identifique claramente su nombre como autor de la misma
b) Comunicar y dar publicidad a la obra en la versión que ceda y en otras posteriores a través de cualquier medio.
c) Solicitar la retirada de la obra del repositorio por causa justificada.
d) Recibir notificación fehaciente de cualquier reclamación que puedan formular terceras personas en relación con la obra y, en particular, de reclamaciones relativas a los derechos de propiedad intelectual sobre ella.

5º. Deberes del autor.

El autor se compromete a:

a) Garantizar que el compromiso que adquiere mediante el presente escrito no infringe ningún derecho de terceros, ya sean de propiedad industrial, intelectual o cualquier otro.
b) Garantizar que el contenido de las obras no atenta contra los derechos al honor, a la intimidad y a la imagen de terceros.
c) Asumir toda reclamación o responsabilidad, incluyendo las indemnizaciones por daños, que pudieran ejercitarse contra la Universidad por terceros que vieran infringidos sus derechos e

intereses a causa de la cesión.

d) Asumir la responsabilidad en el caso de que las instituciones fueran condenadas por infracción de derechos derivada de las obras objeto de la cesión.

6º. Fines y funcionamiento del Repositorio Institucional.

La obra se pondrá a disposición de los usuarios para que hagan de ella un uso justo y respetuoso con los derechos del autor, según lo permitido por la legislación aplicable, y con fines de estudio, investigación, o cualquier otro fin lícito. Con dicha finalidad, la Universidad asume los siguientes deberes y se reserva las siguientes facultades:

- La Universidad informará a los usuarios del archivo sobre los usos permitidos, y no garantiza ni asume responsabilidad alguna por otras formas en que los usuarios hagan un uso posterior de las obras no conforme con la legislación vigente. El uso posterior, más allá de la copia privada, requerirá que se cite la fuente y se reconozca la autoría, que no se obtenga beneficio comercial, y que no se realicen obras derivadas.
- La Universidad no revisará el contenido de las obras, que en todo caso permanecerá bajo la responsabilidad exclusive del autor y no estará obligada a ejercitar acciones legales en nombre del autor en el supuesto de infracciones a derechos de propiedad intelectual derivados del depósito y archivo de las obras. El autor renuncia a cualquier reclamación frente a la Universidad por las formas no ajustadas a la legislación vigente en que los usuarios hagan uso de las obras.
- La Universidad adoptará las medidas necesarias para la preservación de la obra en un futuro.
- La Universidad se reserva la facultad de retirar la obra, previa notificación al autor, en supuestos suficientemente justificados, o en caso de reclamaciones de terceros.

Madrid, a …4….. de ….septiembre……... de …2018

ACEPTA

Fdo…Nuria Cobo-Losey Rodríguez……

Motivos para solicitar el acceso restringido, cerrado o embargado del trabajo en el Repositorio Institucional:

Declaro, bajo mi responsabilidad, que el Proyecto presentado con el título CRUISE-SHIP ENERGY SYSTEM DESIGN AND OPTIMIZATION UNDER UNCERTAINTY

en la ETS de Ingeniería - ICAI de la Universidad Pontificia Comillas en el curso académico 2017-2018 es de mi autoría, original e inédito y no ha sido presentado con anterioridad a otros efectos. El Proyecto no es plagio de otro, ni total ni parcialmente y la información que ha sido tomada de otros documentos está debidamente referenciada.

Fdo.: Nuria Cobo-Losey Rodríguez Fecha: 30/08/2018

Autorizada la entrega del proyecto

EL DIRECTOR DEL PROYECTO

Fdo.:..... Fecha: 2018-09-03

DISEÑO Y OPTIMIZACIÓN BAJO INCERTIDUMBRE DEL SISTEMA ENERGÉTICO DE UN CRUCERO

Autor: Cobo-Losey Rodríguez, Nuria.

Director: Maréchal, Francois.

Supervisores: Moret, Stefano. Baldi, Francesco.

Entidad Colaboradora: École Polytechnique Fédérale de Lausanne (EPFL) .

RESUMEN DEL PROYECTO

Introducción

El transporte marítimo juega un papel crítico en la sociedad de hoy, al permitir cerca del 90% de todo el comercio internacional. La tasa de crecimiento que este sector ha experimentado en las últimas décadas es una de las más dramáticas que se han observado entre las distintas industrias. Dentro del mundo de las embarcaciones, la industria de los cruceros también ha sufrido una importante expansión, habiendo aumentado la demanda de esta más de un 62% entre 2005 y 2015 [1][2][3].

A pesar de su alta contaminación, los motores Diesel siguen siendo escogidos por defecto para la propulsión y generación de electricidad en los barcos, sobre todo por sus ventajas económicas. Por este motivo, sin embargo, los barcos contribuyen actualmente en más de un 3% de las emisiones globales de GEI, emitiendo además una considerable cantidad de materia particulada y otros contaminantes de aire peligrosos. Habiendo aumentado el nivel de conciencia medio ambiental en los últimos años, cada vez más esfuerzos globales están siendo dirigidos a la reducción del impacto de los barcos sobre el medio ambiente. Como consecuencia, la Organización Marítima Internacional (OMI) ya ha anunciado el establecimiento de regulaciones más estrictas sobre las emisiones de los barcos para el 2021 [4][5].

Dado que reducir el consumo de combustible de los barcos conlleva una reducción de sus emisiones, es ahora de interés mundial aumentar la eficiencia de estas embarcaciones. Diversos investigadores están estudiando el mejoramiento de dicha eficiencia, desde por medio de medidas de retrofit hasta el completo rediseño de su sistema energético. Entre las estrategias evaluadas, el uso de tecnologías alternativas, como las celdas de combustible, está siendo percibido cada vez más como la solución energética más prometedora [6].

La mayor parte de estos estudios, sin embargo, optimizan de manera determinista el diseño de sus sistemas propuestos. Esto significa que todos los parámetros de entrada del modelo se asumen conocidos con toda confianza, aún cuando han sido predichos en el largo plazo. No obstante, estos pronósticos frecuentemente resultan ser imprecisos [7]. Como resultado, la presencia de incertidumbre en los modelos de sistemas energéticos es innegable, especialmente cuando éstos incluyen el uso de tecnologías no establecidas, como las celdas de combustible.

Las incertidumbres en los parámetros pueden tener un impacto importante en las soluciones óptimas de diseño. Sin embargo, éstas son raramente consideradas en la optimización de sistemas energéticos

[7][8]. Por esta razón, el objeto de este proyecto es valorar las incertidumbres involucradas en los sistemas energéticos de barcos, basados en el uso de celdas de combustible, para finalmente evaluar la influencia de éstas sobre los resultados de optimización. Además, dado que los cruceros presentan demandas de energía más diversas, haciendo sus sistemas energéticos más complejos, el enfoque de este trabajo se hace sobre dicho tipo de barcos. El objetivo último es dar respuesta a las siguientes preguntas: *¿Qué parámetros de entrada tienen el mayor impacto en el diseño óptimo de este tipo de sistemas energéticos? ¿Cambian mucho los resultados si todos los parámetros se incluyen en el estudio, no sólo un subgrupo? ¿Se seguirían viendo las celdas de combustible como potencial solución energética para los cruceros si todas las fuentes de incertidumbre fuesen tomadas en cuenta?*

Sistema energético estudiado

El análisis descrito se aplica al sistema energético, investigado y optimizado por Baldi en [9], basado en el uso de celdas de combustible y que ha reportado un desempeño energético prometedor. El sistema consiste en una celda de combustible de óxido sólido (SOFC), combinado con componentes auxiliares, que proporciona la energía de un crucero que navega en el mar Báltico. La celda SOFC fue elegida no sólo por su alta eficiencia, sino también por ser apta para la cogeneración. En [9], la hibridación de la SOFC con una celda PEM produjo los mejores resultados en eficiencia, por lo que ha sido dicho sistema, representado en Figura 1, el considerado en este proyecto.

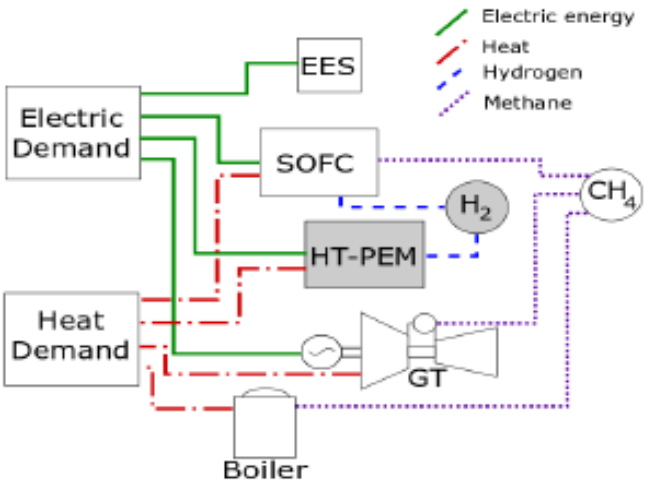

Figura 1: Sistema energético para cruceros estudiado en este proyecto. Extraído de [9].

Dadas las limitaciones en la variación de carga de la SOFC, el sistema híbrido se equipa con tecnologías complementarias: Baterías de ión litio (EES) para transitorios rápidos y peak shaving; una turbina de gas (GT) para cubrir las demandas pico de electricidad; almacenamiento de H_2 para alimentar la celda PEM durante transitorios medios y lentos; y una caldera (GB) para las altas demandas de calor. La distribución de electricidad y la propulsión del crucero se realizan en CC.

El diseño del sistema energético se optimiza por medio de la programación linear entera mixta (MILP), minimizando el coste total del sistema.

Metodología

Para responder a las preguntas anteriormente presentadas, se realizaron los dos siguientes estudios sobre el modelo del sistema energético:

1. **Caracterización de incertidumbre:** La incertidumbre en los parámetros de entrada del modelo es cuantificada. En otras palabras, a los parámetros se les asigna una medida cuantitativa de su incertidumbre, para que su efecto en la optimización pueda ser valorado. Después de filtrar y agrupar los parámetros de manera preliminar, se definen rangos de variación para cada categoría de factores inciertos. A cada una de éstas, se les aplica un conjunto de criterios que ayudan a reconocer las posibles maneras de caracterizar su incertidumbre. Los criterios abarcan desde la colecta de datos históricos o actuales y el uso de pronósticos con sus respectivas precisiones, hasta el desarrollo de modelos. Finalmente, todos los parámetros de entrada son asignados con una distribución uniforme de su incertidumbre.
2. **Análisis de sensibilidad (AS):** Se evalúa el grado de influencia que las incertidumbres previamente medidas tienen sobre el diseño óptimo del sistema y su coste. Esto se consigue mediante un análisis de sensibilidad, un estudio que permite repartir las incertidumbres en las salidas del modelo entre las diferentes fuentes de incertidumbre de las entradas [7]. En este proyecto, se emplea el método de los efectos elementales (EEs), que se encuentra a mitad de camino entre las técnicas globales y locales de AS. El método permite, por un lado, identificar los parámetros no influyentes, clasificándolos según su impacto en una determinada salida del modelo. Por otro lado, sirve para reconocer correlaciones entre entradas y salidas y así verificar la capacidad del modelo para emular el sistema real. Además, para valorar la importancia de incluir todas las fuentes de incertidumbre y no sólo un subgrupo de éstas elegido arbitrariamente, se realizaron dos análisis diferentes. Uno en el que sólo se consideraron los parámetros de costes y otro en el que todos los parámetros inciertos fueron incluidos. El enfoque, sin embargo, se ha hecho sobre el segundo análisis.

Resultados

La caracterización de incertidumbre revela que la entrada con mayor incertidumbre es el precio del gas natural, con un rango de variación de ±50%. Ésta es seguida por los costes de inversión y las eficiencias de las nuevas tecnologías (SOFC y PEMFC), teniendo rangos de ±45% ±35%, respectivamente. Incluso factores relativos a tecnologías convencionales alcanzan valores de incertidumbre de ±30%, como en el caso de los costes de inversión. De todas formas, cabe mencionar, que algunos parámetros inciertos tuvieron que ser excluidos del análisis por limitaciones temporales. Sus incertidumbres podrían ser significativas y deberían ser evaluadas en estudios futuros.

El método EEs se aplicó al sistema energético, tomando el coste total y los tamaños de las tecnologías como las salidas de interés. Los resultados muestran que, si los parámetros se clasifican en base a su influencia sobre el coste total, sólo 10 de los 44 involucrados tienen un impacto de al menos 5% del valor de impacto máximo, tal y como ilustra la Figura 2. Al ser la única fuente de energía del sistema, el precio del gas natural tiene la mayor influencia sobre el coste total. Sin embargo, los tamaños óptimos de las tecnologías sufren efectos más diversos, siendo sus parámetros influyentes más bien diferentes. Las Figuras 3a) y 3b) muestran, por ejemplo, los factores más relevantes para los tamaños de la SOFC y de la turbina de gas, junto con los signos de las relaciones entrada-salida correspondientes.

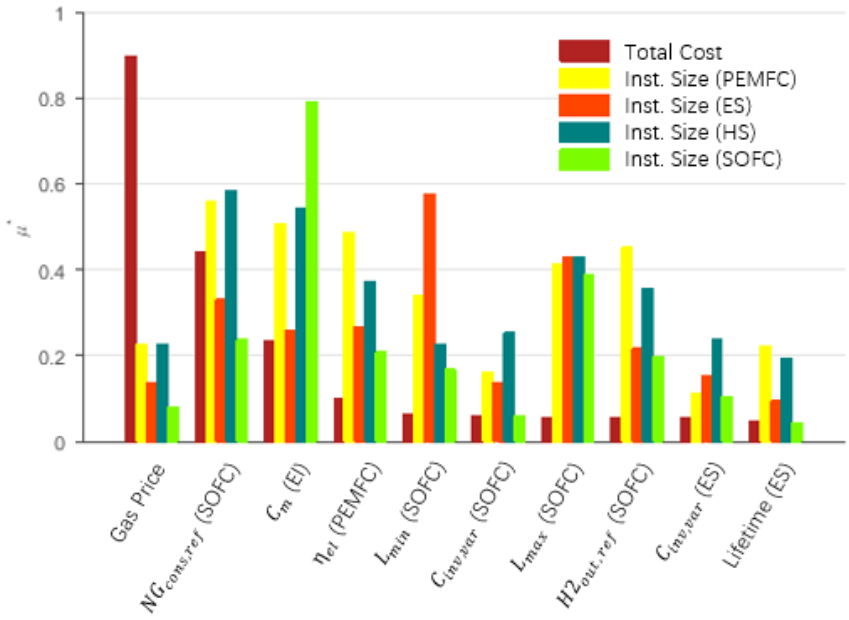

Figura 2: Parámetros de entrada, con sus medidas absolutas de sensibilidad sobre todas las salidas consideradas, clasificados con respecto al coste total del sistema.

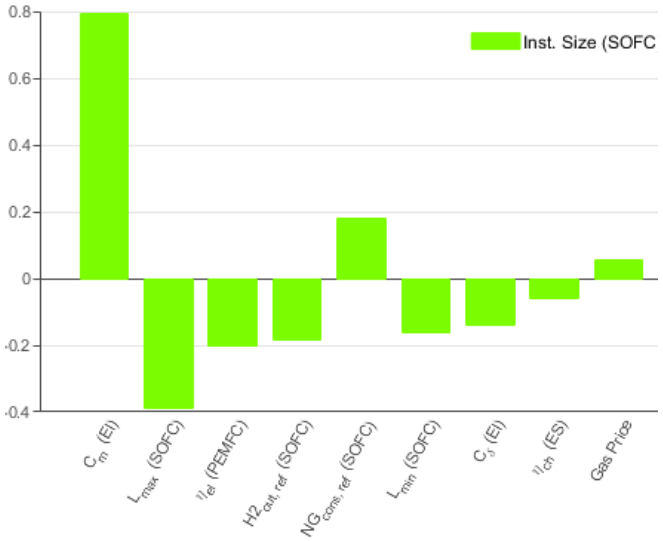

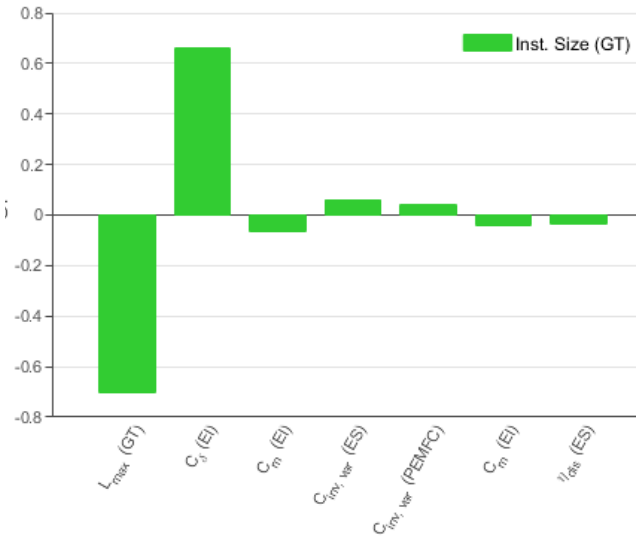

igure 3a): Input parameters ranked on their influence on the size o SOFC.

gure 3b): Input parameters ranked on their influence on the size c GT.

Tal y como se observa en las figuras, un mayor y más variado conjunto de parámetros tienen cierta influencia sobre el tamaño de la SOFC, comparado con el de la turbina de gas. Sin embargo, al no existir una alternativa real a la SOFC (la PEMFC depende de su producción de hidrógeno), su contribución a la generación de energía se mantiene relativamente estable. Mientras que la demanda media de electricidad es el parámetro más importante para la SOFC, éste no tiene un efecto significativo sobre el tamaño de la turbina. En su lugar, es la variación de dicha de demanda la que es uno de los factores mas influyentes para esta última tecnología. En ambos casos, sin embargo, sus respectivas cargas máximas tienen una fuerte relación opuesta a sus tamaños, implicando que cuánto

menos se limita su capacidad de carga pico, menos potencia nominal debe ser instalada. También cabe destacar el hecho de que parámetros relativos a los costes aparecen escasamente en los rankings resultantes.

Conclusiones

La caracterización de incertidumbre y el análisis de sensibilidad realizados en este proyecto permiten extraer algunas conclusiones importantes. Primero, la incertidumbre presente en los sistemas energéticos de cruceros es significativa, especialmente en los factores relativos a las tecnologías más nuevas y a los parámetros de alta variabilidad, como el precio del gas natural. Además, al no ser despreciable para algunos parámetros de las tecnologías convencionales, esto sugiere que hasta la incertidumbre en sistemas energéticos tradicionales es considerable. Segundo, el análisis de sensibilidad permite evaluar el impacto de estas incertidumbres, a la vez que se detectan las que carecen de influencia. Se observa que, aunque la incertidumbre está presente en diversos parámetros, sólo la de unos pocos factores es importante con respecto al coste total del sistema o los tamaños de las tecnologías. Las incertidumbres con mayor impacto son las de parámetros como el precio del gas, la demanda media de electricidad, las eficiencias de las celdas de combustible y sus eficiencias. Al contrario de lo que se suele asumir, la incertidumbre de los costes no tiene un efecto sustancial sobre las salidas del modelo, ni siquiera sobre el coste total. Esto demuestra que, si sólo un subgrupo de parámetros es inicialmente considerado como incierto, los resultados de la relevancia de la incertidumbre podrán ser bastante engañosos.

Referencias

[1] Francesco Baldi. Modelling, analysis and optimization of ship energy systems. PhD thesis, Chalmers University of Technology, 2016.

[2] About the Cruise Ship Industry |http://www.cruiseshipjobsnetwork.com/cruise/cruise-shipindustry/.

[3] Cruise Industry Overview. Technical report, Florida-Caribbean Cruise Association, Florida, 2017.

[4] Miola, A., B. Ciuffo, Giovine, E., and Marra, M. Regulating air emissions from ships. The state of the art on methodologies, technologies and policy options. Technical report, Joint Research Centre Reference Report, Luxembourg, 2010.

[5] S. Brynolf, M. Magnusson, E. Fridell, and K. Andersson. Compliance possibilities for the future ECA regulations through the use of abatement technologies or change of fuels. Transportation Research Part D: Transport and Environment, 28:6–18, May 2014.

[6] Rami El Geneidy, Kevin Otto, Pekka Ahtila, Pentti Kujala, Kari Sillanpaa, and Tero Maki-Jouppila. Increasing energy efficiency in passenger ships by novel energy conservation measures. Journal of Marine Engineering & Technology, 17(2):85–98, May 2018.

[7] Stefano Moret. Strategic energy planning under uncertainty. PhD thesis, Ecole Polytechnique Federale de Lausanne, Lausanne, Switzerland, October 2017.

[8] Georgios Mavromatidis, Kristina Orehounig, and Jan Carmeliet. Uncertainty and global sensitivity analysis for the optimal design of distributed energy systems. Applied Energy, 214:219–238, March 2018.

CRUISE-SHIP ENERGY SYSTEM DESIGN AND OPTIMIZATION UNDER UNCERTAINTY

Author: Cobo-Losey Rodríguez, Nuria.

Supervisor: Maréchal, Francois.

Assistant Supervisors: Moret, Stefano. Baldi, Francesco.

Collaborating Entitity: École Polytechnique Fédérale de Lausanne (EPFL) .

PROJECT SUMMARY

Introduction

Bearing around 90 % of all international trade, maritime shipping plays a critical role in today's society. The growth rate that this sector has experienced in the past decades is one of the most dramatic ones that have been witnessed across all industries. Within the shipping world, the cruise-ship industry has also suffered an important expansion, with its demand having increased over 62% from 2005 to 2015 [1][2][3].

Despite their polluting characteristic, diesel engines are still chosen by default as the means to propel and generate power in ships, mostly for their economic advantages. As consequence, however, ships are contributing in more than 3% to the total global GHG emissions, while additionally emitting a considerable share of particulate matter and other hazardous air pollutants. The level of environmental awareness having increased in the past years, global efforts are being more and more directed towards the reduction of ships environmental impact. Stricter emissions regulations, to be established by 2021, have already been announced by the International Maritime Organization [4][5].

As reducing overall fuel consumption of ships entails lowering their emissions, increasing the efficiency of these vessels is now of global interest. Several researchers are studying the improvement of ship energy efficiency, from retroffiting measures to the complete redesign of their energy systems. Among the proposed strategies, the use of alternative technologies, such as fuel cells, is being increasingly viewed as the most promising energy solution [6].

The most part of these studies, however, are optimizing the design of their proposed systems in a deterministic way. This means that the values of all model input parameters are assumed to be known with complete confidence, even when they have been forecasted on the long term. These forecasts are, nonetheless, often proven to be inaccurate [7]. As a result, the presence of uncertainty in these energy systems' models is undeniable, especially when they include the use of non-established technologies, such as fuel cells.

Input uncertainties can have an important impact on optimal design solutions. However, they are seldom considered in the optimization of energy systems [7][8]. For this reason, the aim of the project is to first assess the uncertainties involved in fuel-cell based ship energy systems and finally evaluate their influence on the optimization results. In addition, as the energy systems of cruise-ships are

particularly interesting for their higher diversity of demand and their complexity, the focus of this work is made on this type of ships.

The objective of this project is to give an answer to the following questions: *What input parameters have the largest impact on the optimal fuel cell energy system design? Do these results change much if all input parameters are included in the study, not only a subset? Would fuel cells still be viewed as a potential energy solution for cruise-ships if all their sources of uncertainty were taken into account?*

Studied energy system

The analysis is applied to a cruise-ship energy system that has been recently proposed, based on the use of fuel cells, reporting promising efficiency performance and with a reasonably competitive cost. This system was investigated and optimized by Baldi in [9], consisting of a solid oxide fuel cell (SOFC) combined with other auxiliary components, that propel and generate power for a cruise-ship that travels daily in the Baltic Sea. An SOFC was chosen not only for its intrinsic higher efficiency but also for its suitability for cogeneration applications. In addition, in Baldi's work, the hybridization of the SOFC with a proton exchange membrane fuel cell (PEMFC) yielded better results on overall efficiency than in the case of a stand-alone SOFC. For this reason, the energy system considered in this project will correspond to Baldi's hybrid system, which is illustrated in Figure 1.

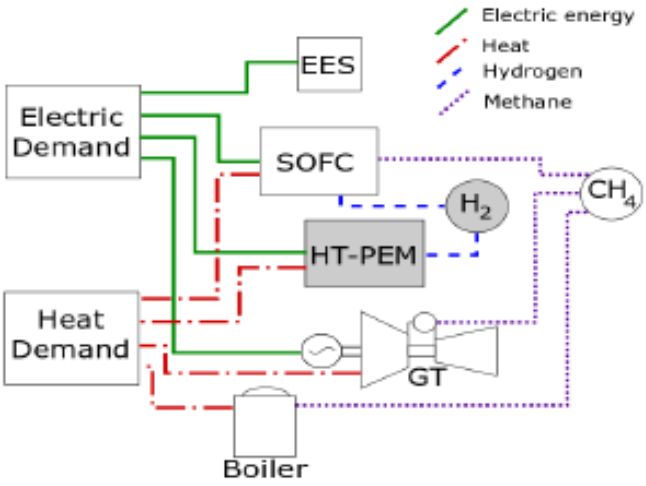

Figure 1: Cruise-ship energy system studied in this project. Extracted from Baldi's work in [9]

Given the load variation limitations of the SOFC, the hybrid system is furnished with complementary equipment: Lithium-ion batteries (EES) for fast transients and peak shaving; a gas turbine (GT) to handle peak electricity demands; hydrogen storage (HS) to feed the PEMFC during medium smooth transients; and a boiler (GB) for extreme heat demands. The whole power distribution and propulsion is assumed to be DC.

In both the work of Baldi and the present one, the energy system is optimized by means of mixed-integer linear programming (MILP), with the total cost of the system as the objective function to be minimized.

Methods

The questions previously presented are addressed applying the two following main steps to the model of the cruise-ship energy system:

1. **Uncertainty characterization**: The uncertainty born by the input parameters of the model is quantified. In other words, parameters are assigned with a quantitative measure of their uncertainty, so that its effect on the optimization can later be assessed. The approach is based, after a preliminary screening and grouping of parameters, on the definition of ranges of variation for all the uncertain factors. A set of criteria are applied to each parameter category that help recognize the different ways in which their uncertainty can be characterized. These range from the collection of historical or current data found in the literature, through the use of forecasts and their associated accuracies, to the development of models. Finally, all input parameters are assigned with a uniform distribution of their uncertainty.
2. **Sensitivity analysis (SA)**: The degree of influence that the measured uncertainties have on the optimal system design and cost is evaluated. This is achieved by means of sensitivity analysis, a study that allows to apportion the uncertainties of model outputs to the different sources of input uncertainty [7]. In this project, the elementary effects (EEs) method is employed, which stands halfway between global and local SA techniques. This method allows, on the one hand, to identify the non-influential input parameters by ranking them based on their impact on a given model output. On the other hand, it serves to recognize input-output correlations and verify the model's capacity to emulate a real system. In addition, to assess the importance of including all input uncertainties and not only an arbitrarily selected subset, two different analysis are made. A first one where only cost-related input parameters are considered and a final analysis where all uncertain factors are included. The focus is, though, made on the latter.

Results

The uncertainty characterization reveals that the input that bears the highest uncertainty is the natural (NG) price, with a range of variation of ±50%. This is followed by the investment costs and efficiencies of newer technologies (SOFC and PEMFC), having ranges of ±45% and ±35%, respectively. Even factors relative to conventional technologies reach values of uncertainty of ±30%, as in the case of their investment costs. It should be noted, though, that a few uncertain factors ended up being excluded from the analysis for time limitations. Their uncertainties, however, could still be significant and should be assessed in future studies.

The EEs method is applied to the energy system, having the total cost, and the technology sizes as the outputs of interest. The results show that, if the input parameters are ranked based on their influence on the total cost, only 10 parameters out of the 44 involved have an impact of at least 5% of the maximum one, as shown in Figure 2. For being the only energy source of the system, the gas price has the greatest influence on the total cost. This factor is followed by the reference fuel consumption of the SOFC and the mean electricity demand. However, the optimal installed sizes of the utilities have more diverse effects, with their influential parameters being rather different. Figures 3a) and 3b) show, as an example, the most relevant factors for the sizes of the SOFC and the GT and the sign of their relationship.

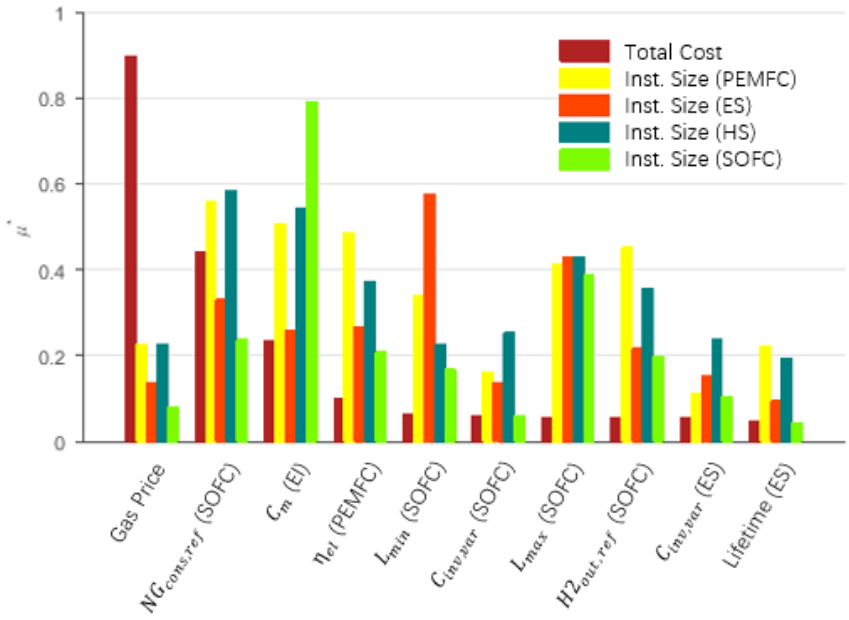

Figure 2: Input parameters, with their absolute measures of sensitivity on all the outputs of interest, ranked w.r.t the total cost.

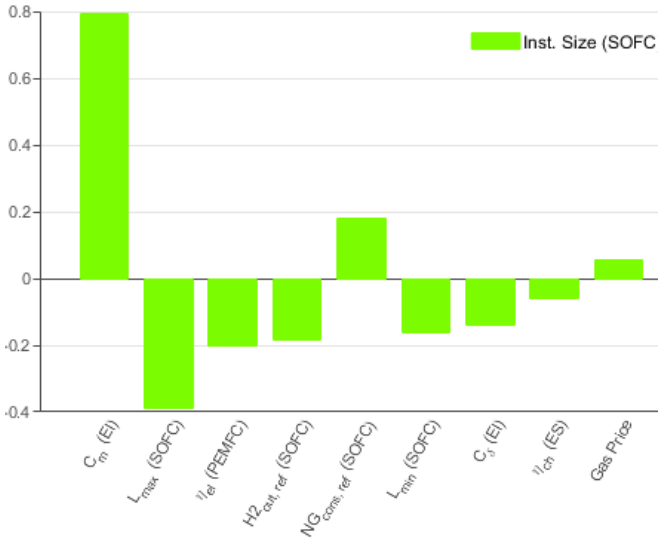

igure 3a): Input parameters ranked on their influence on the size o SOFC.

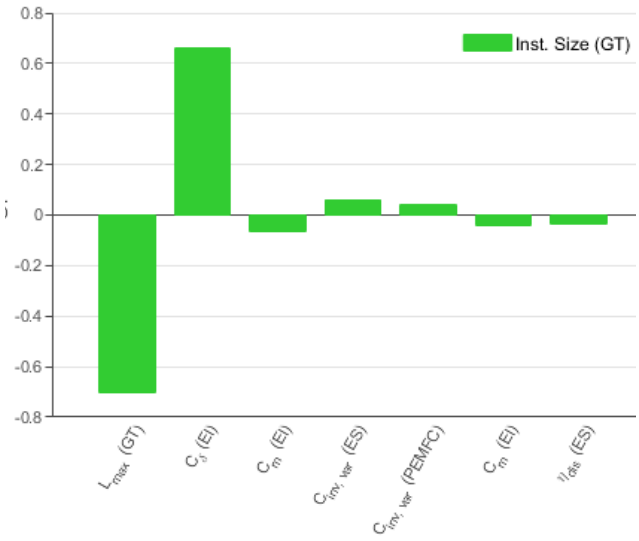

gure 3b): Input parameters ranked on their influence on the size c GT.

As observed, there is a larger and more varied set of input factors that have some influence on the size of the SOFC, compared to the GT's size. However, as there is no real alternative to the SOFC (the PEMFC depends on its hydrogen production), its contribution to energy generation remains close to stable. While the average electricity demand is the most important factor for the SOFC, it has not significant effect on the size of the GT. Instead, it is the variation of this demand that is one of the most influential parameters for the latter technology. In both cases, however, their respective maximum loads have a strong and opposite relationship with their sizes, meaning that the less their

peak load capacities are restricted, the lower nominal power is required to be installed. The fact that the cost-related parameters hardly appear on any of these rankings should also be noted.

Conclusions

The uncertainty characterization and sensitivity analysis performed in this project allow to draw a few important conclusions. First, the uncertainty present in cruise-ship energy systems is significant, especially for factors relative to the newer technologies and for parameters with high variability, such as the NG price. As it is also not negligible for more conventional technologies, this suggests that even the input uncertainty present in traditional energy systems models is meaningful. Second, the sensitivity analysis allows to evaluate the impact of these uncertainties, while also detecting the non-influential ones. It is observed that, even though the uncertainty is present in several parameters, only that of a few factors is important with respect to the total costs and technology sizes. The most impactful ones correspond to inputs such as the gas price, the mean electricity demand, the fuel cell efficiencies and their load limitations. Unlike what is usually assumed, the uncertainty in the cost parameters does not have an important effect on the outputs, not even on the total cost. This shows that if, prior to the analysis, only a subset of parameters is considered as uncertain, the results on the relevance of uncertainty would be quite misleading.

References

[1] Francesco Baldi. Modelling, analysis and optimization of ship energy systems. PhD thesis, Chalmers University of Technology, 2016.

[2] About the Cruise Ship Industry |http://www.cruiseshipjobsnetwork.com/cruise/cruise-shipindustry/.

[3] Cruise Industry Overview. Technical report, Florida-Caribbean Cruise Association, Florida, 2017.

[4] Miola, A., B. Ciuffo, Giovine, E., and Marra, M. Regulating air emissions from ships. The state of the art on methodologies, technologies and policy options. Technical report, Joint Research Centre Reference Report, Luxembourg, 2010.

[5] S. Brynolf, M. Magnusson, E. Fridell, and K. Andersson. Compliance possibilities for the future ECA regulations through the use of abatement technologies or change of fuels. Transportation Research Part D: Transport and Environment, 28:6–18, May 2014.

[6] Rami El Geneidy, Kevin Otto, Pekka Ahtila, Pentti Kujala, Kari Sillanpaa, and Tero Maki-Jouppila. Increasing energy efficiency in passenger ships by novel energy conservation measures. Journal of Marine Engineering & Technology, 17(2):85–98, May 2018.

[7] Stefano Moret. Strategic energy planning under uncertainty. PhD thesis, Ecole Polytechnique Federale de Lausanne, Lausanne, Switzerland, October 2017.

[8] Georgios Mavromatidis, Kristina Orehounig, and Jan Carmeliet. Uncertainty and global sensitivity analysis for the optimal design of distributed energy systems. Applied Energy, 214:219–238, March 2018.

[9] Francesco Baldi, Ligang Wang, and Francois Marechal. Integration of solid oxide fuel cells in cruise ship energy systems.

Contents

List of Tables

List of Figures

Chapter 1: Introduction

1 Introduction

Maritime shipping currently plays a central role in society. Bearing around 90% of all international trade, the shipping industry is the backbone of today's worldwide economies. The growth rate that this sector has witnessed in the past decades is certainly one of the most dramatic ones that have been seen in all industries [6] . Within the shipping world, the cruise sector has also experienced an extraordinary expansion. During the last few years, it has been acknowledged as one of the job sectors that has flourished faster in the world, having an increase in demand of over 62% from 2005 to 2015 and carrying up to 27 million passengers in 2017 [7] [8].

The whole shipping industry, however, is now starting to be hindered by drastic variations of fuel prices, as well as the establishment of rigorous environmental laws. Even though transport by water has been recognized as the cheapest and most efficient way to exchange goods across continents, its environmental impact is not negligible. These ships contribute in a significant share to the emission of anthropogenic greenhouse gases. It has been estimated that their emissions of carbon dioxide (CO_2) and SO_x represent, respectively, 3-5% and 5% of the total global emissions. Their contribution to the emission of particulate matter (PM), volatile organic compounds (VOCs) and hazardous air pollutants is similarly considerable [9]. The level of environmental awareness having significantly increased, ships are now required to become cleaner modes of transport at a global scale.

Despite their polluting characteristic, diesel engines fed by heavy fuels have been and still are currently chosen by default for power generation in maritime applications. The reduced costs of this technology and these fuels is their greatest benefit. However, more rigorous regulations, announced to be established in the next years, aim at reforming this global trend. The international maritime organization (IMO) has informed that stricter emission limits will be set by 2021, especially for emissions of NO_x and SO_x [10].

Improving the energy efficiency of these vessels would entail an overall reduction of fuel consumption, and therefore of emissions. For this reason, the optimization of ships energy systems is increasingly becoming of global interest. Research efforts are progressively targeting the enhancement of energy efficiency of ships, including that of cruise-ships. Both the development of new energy solutions or the upgrade of currently-used technologies have and, still are, being evaluated.

In the cruise-ship field, studied measures have included the combination of dual pressure steam cycles with diesel engines for power production; the incorporation of organic rankine cycles (ORCs) for the recovery of waste heat and efficiency optimization through process integration [11] [3]. The redesign of the whole cruise-ship

energy system has also been investigated, in some cases involving the replacement of diesel engines by gas turbines (GTs), or a combination of GTs with steam turbines. However, newer and cleaner technologies, such as fuel cells, are being viewed more and more as one of the most promising future solutions for onboard power generation. [12] [13].

Among the existing fuel cell types, the Solid Oxide Fuel Cell (SOFC) is now gaining greater attention, as reported in [14]. The interest in this new technology lies on its increased electrical efficiency, its low emissions, its reliability and its high power density. Due to the high temperatures in which they operate, they are also suitable for cogeneration, making them particularly interesting for ships with a diversified energy demand, such as cruise-ships. In fact, a recent study has evaluated the performance of an SOFC-based cruise-ship energy system, both in the case of a stand-alone SOFC and in combination with a proton exchange membrane fuel cell (PEMFC). The obtained results were satisfactory for both cases, but especially in the hybrid system, where efficiencies of up to 70% were reported [3].

These new energy solutions, together with the stricter demands on ships' environmental impact, are increasing, however, the complexity of these vessels' energy systems. As a result, the importance of proper technology selection, integration and sizing is also rising.

The common strategy in the design optimization of energy systems is to take a deterministic approach. This means that all input parameters are assumed to be known with complete confidence, even if they have been forecasted on the long term. These forecasts are, nonetheless, frequently proven to be inaccurate. For instance, in the prediction of natural gas prices, overestimations by a factor of 3.32 and underestimations by a factor of 2.95 have been reached in 1995 and 2005, respectively [15]. These values serve, thus, to confirm that the uncertainty involved in energy systems models can be significantly high.

Despite the clear presence of uncertainties in the inputs of energy systems models, they are seldom considered in the design optimization of these systems. In addition, in most cases, only a small subset of input parameters are assumed as uncertain, prior to any analysis. However, the impact that these uncertainties, and those that are disregarded, have on the optimal solutions can be considerably important [16].

2 Objectives

The aim of this project, in general terms, is to study the uncertainty involved in and its influence on the design optimization of ship energy systems. Although there are one hundred times more merchant vessels than cruise-ships [17][18], the latter are particularly interesting from the research perspective. Having to supply electricity and heat for all the hotel services they provide, the auxiliary power demand of cruise-ships is significantly higher than in commercial vessels. In fact, as will be detailed next, the electricity and heat demands of cruise-ships are comparable to their propulsion needs, hence making their energy systems more complex. It is for this reason that the focus of this work will be made on the energy systems of these ships.

As previously stated, fuel cells are being more and more perceived as the promising solution for cleaner cruise-ship energy supply. In addition, recent studies are already endorsing this idea by reporting exceptional efficiency performance of these technologies and with competitive costs. Such is the case of the research carried out by Baldi on an SOFC-based cruise-ship energy system, aforementioned [3]. Fuel cells, however, are still facing manufacturing challenges and are yet to be produced in large scales. Thus, their characteristics and costs are most likely subject to considerable uncertainties, larger than more conventional technologies. These studies, nonetheless, have not accounted for these or any other relative uncertainties, including the work of Baldi.

The objective of this project will therefore be to assess the input uncertainties present in fuel-cell-based cruise-ship energy systems and how these affect the optimal system design. To do this, the energy system proposed and optimized by Baldi will be used as the case study to which the analysis is applied. After the study, it should be possible to answer the following questions:

What input information have the largest impact on the optimal fuel cell energy system design? Do these results change much if all input parameters are included in the study, not only a subset? Would SOFCs still be viewed as a potential energy solution for cruise-ships if all their sources of uncertainty were taken into account?

To achieve this, the uncertainty born by all parameters that are input to the energy system model will be quantified. In other words, they will be assigned with a quantitative measure of their uncertainty. This step is named, here, as the uncertainty characterization. Once the present uncertainties have been quantified, their impact on the optimal design and its cost will be assessed. This will be achieved by means of sensitivity analysis, with the application of the elementary effects method, which will be described next. The sensitivity analysis will allow not only to identify the

most influential parameters of the energy system model, but to recognize input-output correlations. This will have the additional benefit of confirming that there are no major mistakes in Baldi's model.

The results obtained in this work will not only serve to evaluate the effect of uncertainty on the given SOFC-based cruise-ship energy system, but will also allow to present a general view on the relevance of uncertainty on other non-established energy technologies. In addition, the characterization of the involved uncertainties will be possible to be used as a reference for future related studies.

3 State of the Art

Among all ship types, cruise-ships are considered to be, from a research point of view, particularly interesting. Compared to cargo vessels, cruise-ships have a more varied energy demand. The main difference is that their auxiliary energy demand is significantly higher, both in terms of power and heat. The total energy demanded by all the onboard services provided for passenger entertainment and comfort, including the HVAC and hot water systems, reaches values comparable to propulsion energy. As noted by Marty *et al.*, the proportions of energy allocated for propulsion and auxiliary electrical demand in a reference trip correspond to 59% and 41% The share of total heating demand remains in the same range of values [19]. Even in the case of smaller cruise-ships, similar ratios have been reported. For instance, the shares of propulsion, electricity and heat demand of a small cruise-ship's average yearly demand, obtained in [20], were 41%, 25% and 34%, respectively.

The energy demand of cruise-ships is also considerably variable, as it is directly influenced by weather changes and variations in the operation of the ship. Lastly, cruise-ships, as for any other boat, can only rely on their own onboard energy system for satisfying their energy demand. Cruise-ships have no resource network that can help them in the fulfillment of their energy requirements [3].

As stated earlier, the contribution of cruise-ships to GHG emissions is not negligible. In fact, it makes up 0.2% of all global carbon dioxide emissions from fossil fuel combustion and cement production [21]. In addition, the amount of particulate matter that cruise-ships emit daily is equivalent to the emissions of 1 million cars [22].

Aiming at reducing the environmental impact of the cruise-ship industry, several measures for improving the energy efficiency of these ships have been studied in recent years. Some of these investigations are presented next in Section 3.1, including the research efforts made on the use of fuel cells as possible solution. Since the present work is focused on an SOFC-based energy system solution, a review of this technology is also presented in Section 4.2.1. Finally, an overview of the studies that have been made regarding uncertainty in energy systems design is provided in Section 3.3

3.1 Increasing efficiency in cruise-ships

Researchers have evaluated the potential of various energy solutions for reducing emissions and fuel consumption of cruise ships. These include strategies such as employing hybrid power, recovering waste heat, achieving higher efficiency in propulsion, among others [23]. According to a review published by Bouman and Lindstad [23], among these approaches, the use of hybrid power for both auxiliary energy

and propulsion could lead to reductions of emissions of up to 20-30%. Efficiency increasing devices, however, have already been largely improved in the past decades and their potential for further improvement remains marginal.

Substituting the currently used Internal Combustion Engines (ICEs) by Gas Turbines (GTs) has also been evaluated in [24] for large cruise ships. Even though gas turbines are known to have lower electrical efficiency compared to ICEs, the benefit gained from cogeneration could possibly eliminate the gap between both propulsion efficiencies. Even though it was shown that cogeneration would not suppose an increase in efficiency large enough to beat the ICEs, gas turbines would still bring benefits in terms of environmental impact (NOx, CO, HC emissions), volume and weight. In addition, it was revealed in [12] that gas turbines could have a brighter future in cruise ships if they were combined with steam turbines, allowing to obtain overall efficiencies of up to 72%.

Interesting measures for retrofitting existing cruise-ships have also been proposed. For instance, the integration of a regenerative Organic Rankine Cycle (ORC) into the energy system of a cruise ship for recovering the waste heat of exhaust gases was presented in [25]. This additional component was proved to be able to supply up to 22% of the total power, reducing fuel consumption in a significant share. Similarly, the use of conventional technologies such as dual-pressure steam systems has also been shown to have a positive effect on their overall efficiency, especially when used in cruise-ships propelled by four stroke Diesel engines [11]. In fact, these systems are already available and have been implemented in various maritime engine applications [11].The work of [26] examined the advantages of improving the loading conditions of an existing cruise-ship's engines by coupling a shaft generator to them.

3.1.1 Use of fuel cells

Among the several approaches for reducing shipping emission levels, fuel cells are viewed as one of the most promising future solutions [13]. The most distinctive feature of fuel cells is their high electrical efficiencies, estimated to reach values of over 70 %, especially when combined with GTs or reciprocating ICEs [27]. They allow to distribute the generation of power within the ship, reducing electricity transport losses and improving redundancy, while maintaining fuel consumption [28]. In addition, their low emissions, decreased noise and vibration, their modularity and reduced maintenance requirements, make fuel cells particularly interesting for maritime applications [14].

Fuel cells have been seen, for decades, as an alternative to heat engines in the maritime field. PEM fuel cells started being developed by the German Navy, in the 1970s, as a propulsion system for submarines that did not depend on air. Air independent propulsion also motivated Adams [29] and Sattler [30] to evaluate the

application of fuel cells in naval submarines. Adams affirmed that the power generation efficiency of fuel cells can be twice as high as that of diesel generators. Sattler, on the other hand, documented a range of efficiencies, from around 40% in the case of PEMFCs working on reformed hydrocarbons, to almost 60% for SOFCs fuelled with natural gas.

Studies and projects have also been carried out for surface vessels. In [31], the United States Coast Guard (USCG) studied the replacement, for one of its vessels, of its four main diesel generators with Molten Carbonate Fuel Cell (MCFC) modules. The fuel cell system generated electricity for both propulsion and power. The installation and operation of the vessel was succesful, and its autonomy was improved thanks to the MCFC's high efficiency, estimated at 54%. SOFC modules, powered with methanol, were installed on board of a merchant vessel in [32]. In this case, however, the fuel cells were only used to supply electricity, not for propulsion.

In general, most past and current projects only consider fuel cells for onboard power supply. Another example is the project by Foss Maritime involving the development of a portable hydrogen fuel cell for providing additional power to docked or anchored vessels [33]. Moreover, scarce information is found in the literature about fuel cell applications for cruise-ships. In 2017, however, the famous cruise-ship company Royal Caribbean announced that a fuel cell was going to be installed and tested in one of their luxury vessels. Although the device would be used to take up part of the hotel load, its suitability for propulsion applications could also be evaluated further in the future [34].

3.2 Solid Oxide Fuel Cell (SOFC)

In recent years, SOFC technology has been gaining more attention in the maritime field for its high projected efficiencies [14]. In fact, in a study carried out by Leites *et al.* [35], it was concluded that SOFCs are favourite among fuel cells for their intrinsicly higher efficiencies and their simpler requirements for auxiliary components.

A solid oxide fuel cell, as any other type of fuel cell, is a device that produces electricity by converting the chemical energy of a fuel through oxidation. It allows to generate electricity both at high temperatures and with low levels of pollution. The main difference with other fuel cells is that the SOFC has a solid oxide or ceramic electrolyte, as indicated by its name. In addition, its modularity, reliability and fuel adaptability contribute to making the SOFC one of the most promising technologies for clean energy production [36] [4] [37].

3.2.1 How it works

A SOFC consists of a dense, oxide ion conducting electrolyte that separates two porous electrodes. Oxygen is supplied to the cathode, known as the air electrode, to react with electrons that come from the external circuit. As a result, oxide ions are produced. These diffuse through the oxide ion conducting electrode until reaching the anode, which is the fuel electrode. At this point, the H_2 (and/or CO) present in the fuel combine with the oxide ions, forming H_2O (and/or CO_2). The electrons released in the reaction then flow from the anode to the cathode, through the external circuit, producing electricity. The described operating principle is depicted in Figure 1 [4].

The electrolyte in SOFCs is commonly made of Yttria-doped zirconia (YSZ), for its chemical stability, adequate ionic conductivity and mechanical strenght. The anode, on the other hand, is required to be highly porous to guarantee that fuel can flow towards the electrolyte. For this reason, it is usually made of granular matter. The cathode must also be a porous, stable microstructure, as it has to allow the gaseous oxygen to migrate to the cathode/electrolyte interface [4].

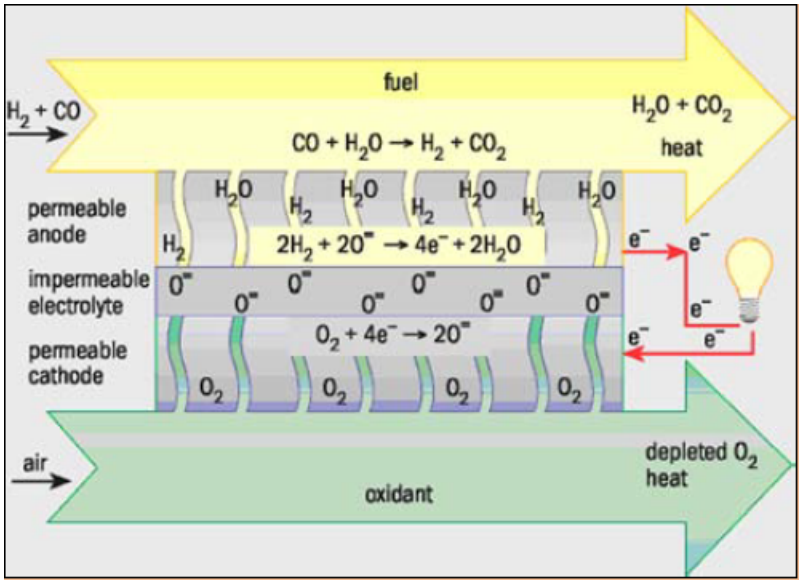

Figure 1: Operating principle of a SOFC. Extracted from [4]

In order to reach higher outlet voltages, multiple cells are connected in series, forming an SOFC stack [37]. The ceramic materials, of which the SOFC is made, only become ionic and electrically conductive once very high temperatures are reached. This conditions SOFC stacks to operate at high temperatures, that range from 500 to 1000 °C. For operating under this thermal conditions, its con-

struction materials must fulfill stringent requirements [38].

3.2.2 Advantages and features of current SOFCs

Compared to conventional technologies for power generation, SOFCs offer considerable advantage in various aspects. As mentioned earlier, these fuel cells are capable of generating electricity at high efficiencies, greater than most traditional technologies. Since the efficiency of SOFCs is not limited by the Carnot cycle of a heat engine, higher values can be reached. Efficiencies of over 60% have already been achieved since 2009 [38] [36]. Furthermore, the high operating temperatures of SOFCs allow them to provide high quality exhaust heat, making them very suitable for cogeneration applications. By using them for combined heat and power applications or with heat engine energy recovery devices, the overall efficiency of SOFCs can be further improved. In fact, efficiency values of up to 85-90% have already been obtained with a CHP system [39] In addition, SOFCs can also be coupled with gas or steam turbines to produce high efficiency combined cycles [36] [40]. As presented in [41], a GT-SOFC hybrid system can reach electrical efficiencies of up to 70%.

Similarly to most fuel cells, SOFCs are modular and scalable. This not only increases the reliability of the technology but also allows for its maintenance to be performed by modules. Moreover, SOFCs' emission levels (only of SOx, NOx and PM) are significantly low, compared to conventional technologies [38].

Relative to other types of fuel cells, SOFCs are fuel adaptable. Again due to its high operating temperatures, methane or other light hydrocarbon fuels can be reformed internally. Carbon monoxide is also accepted as fuel, and some concentration of impurities is tolerated. This includes typical fossil fuel impurities, such as chlorides and ammonia [40].

The severe thermal stresses, caused by the high temperatures and suffered by the construction materials, limit the life of the SOFC systems. Nonetheles, a runtime record of continuous operation during 10 years of such a system has been registered [42]. In general, a system duration of 40000 hours is considered to be a feasible objective for SOFC technologies [43].

3.2.3 Hybridization with PEMFCs

An SOFC's capacity to internally reform can be beneficially exploited by combining it with a proton exchange membrane fuel cell (PEMFC). This type of fuel cells are characterized for operating at low temperatures (between 50 and 100°C) and having a polymer membrane that conducts protons as the electrolyte. In addition, they work on fuels with high contents of hydrogen, which can be produced from other fossil fuels by reforming and shift reactor processing [44]. In a combined SOFC-

PEMFC system, the SOFC's exhaust stream of reformate gas can be processed by shift reactors and fed directly to the PEMFC. Additional power is thus generated while eliminating the need of a reformer upstream of the PEMFC. As a result, the overall efficiency of the system is increased [45].

SOFC-PEMFC systems have been described and analyzed in the literature. The conceptual design of such a system was initially introduced by Dicks *et al* in 2002 [46]. In this study, the overall efficiency of the combined system was forecasted to be of 61%, higher than the stand-alone values at the time. Yokoo *et al.* [47] proposed a SOFC-PEMFC system configuration, with parallel fuel feeding, the efficiency of which resulted to surpass by 5 % that of the stand-alone SOFC. Moreover, in the work of[48], a 1472-kW SOFC-PEMFC hybrid system design was optimized using a multi-objective strategy. In this case, the results revealed that an overall efficiency of 73 % was the maximum attainable [49].

A combined heat, hydrogen and power generation system, incorporating the two fuel cells in question, was studied by Becker *et al.*. In their design, the SOFC was coupled with 1- or 2-stage gas shift reactors, followed by a PSA or membrane technologies for hydrogen upgrading [1]. This system is now being designed, and will be exposed in EU H2020 project CH2P, to supply refilling stations of hydrogen and electricity [50].

3.3 Uncertainty assessment in energy systems design

The design and optimization of energy systems is commonly performed under deterministic assumptions. The models used do not consider uncertainty and are often based on long-term estimations for key parameters. However, forecasts have been proved to be frequently mistaken, leading to inadequate or suboptimal installed technology sizes and deficient system operation.

Uncertainties involved in the input parameters are inherent to any energy system model and have an important impact on their design optimization. However, to date they are seldom integrated in optimization models. Keirstead *et al.* [51] remarks, in a review of current models for urban energy systems, that the presence of uncertainty was only mentioned in three of the reviewed works, out of a total of 219. G. Mavrornatidis *et al.* also highlight the extensive current use of deterministic approaches in distributed energy systems design [16]. Similarly, very few (or even none) studies, accounting for uncertainty in the design of a ship's energy system, can be found in the literature.

The obstacles behind the consideration of uncertainties in process systems engineering, that prevent a wider spread of this practice, have been identified by Grossmann

et al. [52]. These include the high computational cost of energy models; the question of measuring input uncertainties and establishing their nature; and the choice of adequate approaches to the incorporation of these uncertainties in energy models. These challenges are, therefore, inevitably faced by all energy system applications, including ship energy system design.

There are two main strategies for assessing the impact of uncertainty in optimization models: sensitivity analysis and optimization under uncertainty, where the uncertainty is directly incorporated into the optimization process. In the present project, however, the focus is made on sensitivity analysis methods.

A necessary step, common to both approaches, is the measurement of uncertainties present in the inputs, here denominated as uncertainty characterization. To be able to account for input uncertainty in energy models, it is first required to quantify it. The way uncertainty is measured can have a considerable effect on the model outputs, or in the uncertainty assessment results. In similar fields, such as energy planning, varied methods have been employed for this matter, including the assignment of ranges of variations and the generation of Probability Distribution Functions (PDFs)[53] [54]. Nonetheless, in most energy modeling practices, the characterization of uncertainty is often given very little importance. In addition, its application is usually reduced to a smaller group of input factors, chosen by the modeler. The difficulty to find relevant and reliable information in the literature may discourage more elaborate characterizations of uncertainty.

Sensitivity analysis (SA) consists of the investigation of how the different uncertainty sources found in the inputs of a mathematical model correlate with the uncertainty in the outputs [5]. This study requires the execution of the deterministic model for multiple distinct scenarios, where the input parameters are sampled from their uncertainty distributions. The computational expense inevitably involved is another reason why these practices remain considerably neglected. As stated in [51], sensitivity analysis is rarely implemented in energy models. A few recent studies, however, have applied SA techniques such as the Monte Carlo or the Morris methods, to the design optimization of distributed energy systems [16] . SA has also been recently used in the optimization of district cooling systems [55].

Chapter 2: The Model of the Energy System

4 Description of the Model

In Baldi's work, the design of the SOFC-based cruise-ship energy system, together with its annual operation, is optimized by means of mixed integer linear programming (MILP). In this project, the problem is adressed similarly, having the objective of minimizing the investments and operational costs of the ship. The physical model of the energy system used in both studies is detailed in this chapter, starting with a general description of the system in Section 4.1. In Section 4.2, the operating mode of the fuel cells and the specifications assumed for all technologies are presented. Further, the case study for which the energy system model is designed, is detailed in Section 4.3. Finally, the complete formulation of the MILP problem is given in Section 4.4.2.

4.1 Proposed Energy System

As previously mentioned, the energy system proposed by Baldi is based primarily on the use of SOFCs as the ship's energy supply option. Given their capacity for flexible combined generation of power, heat and hydrogen, these fuel cell systems allow their hybridization with batteries and PEMFCs. Since SOFCs cannot bear strong variations in load, these complementary technologies are included to respond to fluctuations in the power demand. As a result, the energy storage capacities of the PEMFC and the batteries make it possible for the SOFC to be operated at almost constant load, guaranteeing an optimal efficiency and durability of the system.

Further, a Gas Turbine (GT) is incorporated to cover high power demands. Although diesel engines have lower running costs and are more simply operated, gas turbines are chosen over them to serve this function. This is because of their higher power density, their better suitability for using natural gas as fuel and their lower emissions. The gas turbine, together with the PEMFC, is considered to work in cogeneration mode, supplying a portion of the heat demand. However, a Gas Boiler is also included to ensure peak heat demands are always covered.
To summarize, the proposed energy system is composed of:

- A SOFC as the base-load energy supplier
- A HT-PEMFC together with a Hydrogen Storage System (HS) for medium-smooth transients
- A Gas Turbine (GT) to handle peak loads of electricity demand
- A Boiler for extreme loads of heat demand
- Electrical energy storage (EES), i.e. batteries, for fast transients and peak shaving

Figure 2 illustrates the energy system, including an indication of the energy streams that are transferred between the different components and which are ultimately converted into electrical energy or heat.

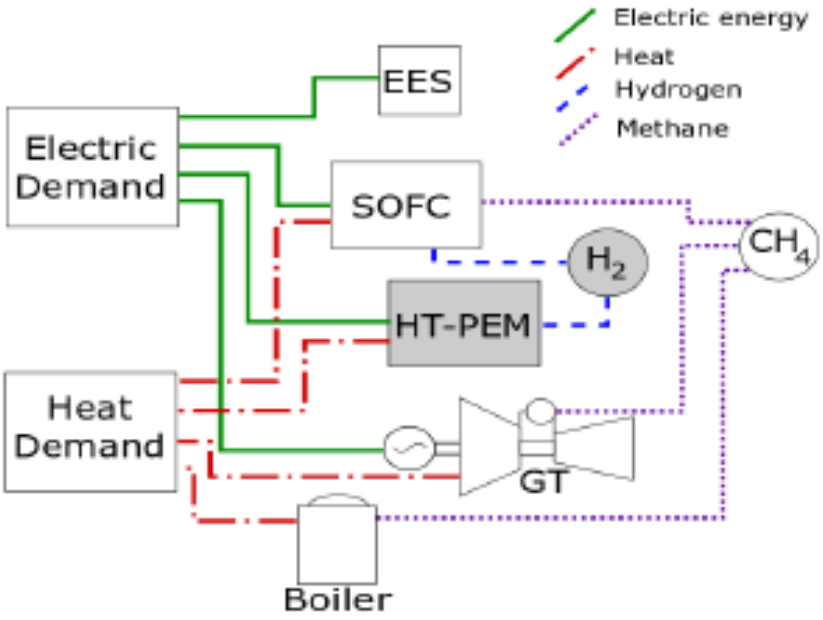

Figure 2: Diagram of the proposed energy system [3]

Given this energy system, the power distribution system of the boat was assumed to be DC. In consequence, it was not necessary to include an inverter in the model, and the propulsion of the ship was considered to be carried out by DC motors. The electric generator of the gas turbine is also assumed to be DC.

4.2 Component Modelling

4.2.1 Solid oxide fuel cell (SOFC)

The solid oxide fuel cell system considered in [3] is based on what Becker et al. proposed in [1]. In such combined heat, hydrogen and power (CHHP) system, a few processes are incorporated after the SOFC to enhance the hydrogen and heat production. A fraction of the unconverted gas coming out of the SOFC is taken to water-gas shift reactors to increase the hydrogen content. A pressure swing absorption (PSA) unit is subsequently used to upgrade the hydrogen mix, obtaining high H_2 purity. On the other hand, additional heat is generated by combusting the unreacted gas from the PSA, which can be used to supply heat to both the system and/or the load. The operational data of the different streams is gathered in Table 1.

Although the system proposed by Becker et al. can be operated in either baseline

mode or hydrogen-overproduction mode, only the latter operating mode is considered in this study. In this case, the fuel input is increased to raise the production of hydrogen, maintaining the same outputs of heat and power as in the baseline mode. The proportions of generated power and hydrogen are, however, assumed to be fixed.

Stream	**Type**	$\dot{H}$ [kW]	T_{in}[K]	T_{out}[K]
Electric net power output	Electricity	1026	-	-
Heat output	Flue gas	311	495	388
Heat output	Fuel mix	106	617	375
Hydrogen output	H_2	333	-	-
Fuel input	CH_4	2084	-	-

Table 1: Operational data of the SOFC system, working in H_2 overproduction mode. Extracted from [1].

In [1], the designed CHHP system resulted to have, at optimal load, a net electric efficiency of 67%. In Baldi's work, however, this value is reduced to 60%, to account for the performance of the SOFC in a wider load range (around the optimal operating point).

4.2.2 High temperaure proton-exchange membrane fuel cell (PEMFC)

In comparison to SOFCs, PEM fuel cells are associated with much lower temperatures of operation. This allows them to adapt to load variations and, therefore, they exhibit a better transient performance than SOFCs [14]. This capacity to deal with load fluctuations is not, however, the only interest behind their use in this energy system. They also represent a means to recover energy. Moreover, their combination with hydrogen storage allows to store energy and produce extra power whenever its needed.

PEM fuel cells work on hydrogen-rich fuel feeds, which can be produced from other fuels (e.g. natural gas) by reforming and shift reactor operations. Since SOFCs are able to reform internally, the stream of reformate gas they generate can be recovered and transformed as described in Section 4.2.1 to obtain highly pure H_2. Hence, fueling PEMFCs with this by-product should result in an enhanced system efficiency [46].

Finally, PEMFCs are also chosen for their higher resistance to carbon monoxide impurities in the fuel feed and their possibility to cogenerate. The operational data considered for this technology is extracted from [2] and gathered in Table 2. It is important to mention that both fuel cells are assumed to be linearly scalable, without

Stream	**Type**	$\dot{H}$ [kW]	T_{in}[K]	T_{out}[K]
Electric net power output	Electricity	1.49	-	-
Heat output	Flue gas	0.54	423	303
Fuel input	CH_4	2.48	-	-

Table 2: Operational data of the PEMFC considered in the energy system. Extracted from [2].

affecting their thermodynamic performance and to have constant, load-independent efficiency.

4.2.3 Units for energy storage

In Baldi's work, the load accepted by the SOFC is, as will be described in Section 4.2.5, bounded within a given range to ensure optimal operation. Hence, this constraint makes necessary the incorporation of energy storage units so that all values of energy demand outside this range can also be covered. The two forms of energy storage that are considered are electric energy and hydrogen, as mentioned in Section 4.1.

Lithium-ion batteries are chosen for the proposed energy system, as they are commonly used in marine installations [56]. No inverter losses are considered in the model of these batteries, and the charging and discharging efficiencies are assumed to be 0.926 and 0.975, respectively [57]. In addition, they are modeled with a depth of discharge (DoD) of 70% [56].

For the hydrogen storage, on the other hand, the auxiliary power requirements are accounted for in its charging and discharging efficiencies. These are both assumed to take a value of 0.98 [57].

4.2.4 Other components

The gas turbine, besides generating power, is also assumed to be capable of producing waste heat of high quality. The considered stand-alone gas turbine is modeled as a utility with constant electrical and thermal efficiencies of 0.33 and 0.6, respectively. In this case, the electrical efficiency is lowered since the gas turbine is mostly used at suboptimal loads. A conservative value is therefore chosen to account for its loss in performance during part-load operation. For the cogeneration, it is assumed that exhaust gases transfer heat from 400 °C to 120 °C. Finally, the associated electric generator is assumed to have an efficiency of 0.95.

4.2.5 Load limitations

Working at very high temperatures, the SOFC technology presents a restricted capacity to vary its power production and adapt with ease to the fluctuating ship load. For this reason, this component is modeled including a load variation constraint (see (1)), that imposes the change of power production between one time step and the following one to be smaller than a certain maximum value. In Baldi's work a 500 kW load variation limitation is considered, as indicated in Table 3, representing between 5% and 20% of the SOFC's installed power.

$$P_{u,t} - P_{u,t+\Delta t} \leq \Delta P_{max} \tag{1}$$

Some additional load constraints were included for the SOFC and other components, such as the gas turbine. In order to maintain an elevated efficiency of the fuel cell, it was assumed to be operated only under a load between 70% and 90% of the installed capacity. The gas turbine, on the other hand, was allowed to run within a wider load range: [10%,100%], to take advantage of its good adaptability. These assumptions are gathered in Table 3.

Stream	**Minimum Load**	**Maximum Load**	ΔP_{max} **[kW]**
SOFC-Polygen	0.7	0.9	500
Gas Turbine	0.1	1	0.6

Table 3: Load limitation assumptions of some of the ships components [3]

4.2.6 Summary data table

Table 4 gathers all the values of the main parameters that are needed to interpret the results of the study, given in Section 5: the maximum power or energy considered for each technology, as each of the technologies' multiplication factors (some of the outputs studied) needs to be multiplied by this parameter, in order to obtain the installed size; and the efficiencies of the different components, for their relevance in the final distribution of power and heat generation among them.

4.3 Case Study

The energy system proposed in [3] and described in Section 4.1 is designed and optimized for the case of a ship currently in operations: A small cruise-ship that sails in the Baltic Sea in daily journeys.

Technology	**Maximum Power/Energy* (kW/kWh)**	**Electrical Efficiency**	**Thermal/Mech* Efficiency**
SOFC-Polygen	10000	0.6	-
HT-PEMFC	2000	0.52	0.12
Hydrogen Storage	50000*	-	0.98*
Batteries	25000*	Ch:0.926/ Disch:0.975	-
Gas Turbine	30000	0.33	0.6
Boiler	4000	-	0.92
Electric Generator	40000	0.95	-

Table 4: Power and efficiency values considered in [3]. The asterisks indicate which of the values of the second column are measured in kWh, and which of the fourth column correspond to a mechanical efficiency.

4.3.1 Ship description

The cruise-ship, being 176.9 m long and having 28.6m of beam, can carry up to 1800 passengers and sail at a cruise speed of 21 knots. The varied set of amenities installed in the ship, coupled with its sizable HVAC system, make its auxiliary energy demand considerably larger than that of a typical cargo vessel, as well as more diverse.

The existing cruise, is propelled by eight Diesel engines: four main engines of 5760 kW each and four supplementary engines, each of 2780 kW. Six exhaust gas boilers and two oil-fired boilers, combined with a system that recovers the engine cooling waste heat, serve to meet the heating demand. In this study, a newly built cruise-ship, having similar dimensions and meeting comparable energy demands, is considered.

4.3.2 Energy demand profiles

The energy demand considered in Baldi's work is based on the work proposed in [20]. Since the studied ship is propelled by electric motors, only two forms of energy demand are found: electricity and heat. As a result, the total electrical demand is an aggregation of the propulsion power and the electrical power supplied to all the different commodities. The heat demand, on the other hand, is composed of both the hot water heating and the HVAC system's demands, the former representing the largest share of the annual heat demand of the existing ship. The distribution of heat on the ship is assumed to be carried out by hot water, having a maximum temperature of 90°C and temperature drop of 20°C. As opposed to the work of [20],

the demands involved in the heating of the fuel tank or for pre-injection are excluded in Baldi's study, since methane does not require to be heated at high temperatures.

The considered energy demand, instead of being analyzed over a full year of operations, was clustered into the demands of four characteristic days, following the suggestions in [58]. Three of these correspond to distinctive days of typical ship operation, each of them belonging to a different season to have larger variation of heat demand. The last day, however, represents a day of extreme electrical demand. In addition, an occurrence rate is assigned to each of these days, to weigh their corresponding recurrence over the whole year in the optimization problem.

The final heat and electrical demand curves are displayed in Figure 3. The annual mean and total values of both energy demands, as well as their respective maximum values are given in Table 5.

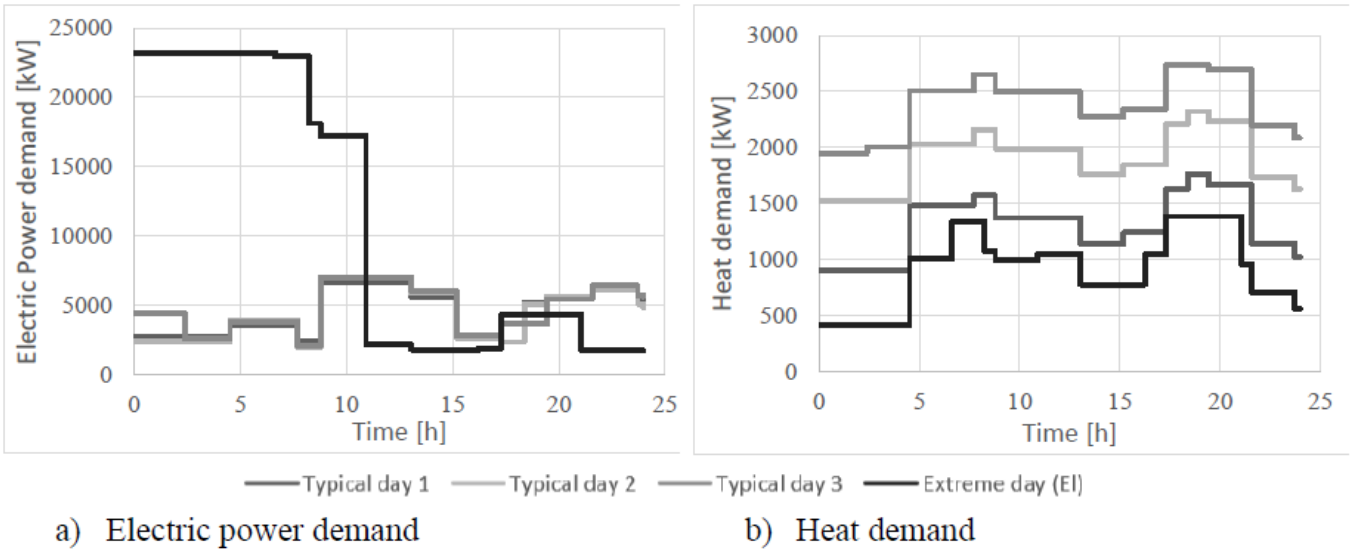

Figure 3: Curves of the two energy demands considered in [3]

	Mean demand (kW)	**Maximum demand (kW)**	**Total demand (GWh/y)**
Electricity	4530	23230	37.4
Heat	1712	2915	14.1

Table 5: Mean, maximum and total values of the considered electrical and heating demands.

4.4 Optimization

The design of the proposed energy system (i.e. the sizes of the different technologies and their operations) is optimized with the help of process integration (or pinch analysis) techniques. The pinch analysis approach is usually used to design or improve the energy efficiency of complex processes, studied as a whole, by optimizing energy recoveries, operating conditions and energy supply methods, with the ultimate objective of minimizing the costs of the system [59] [60]. In the present work, the interest does not lie on optimizing any complex processes, rather, on designing an optimal utility system that supplies the energy demand of the ship. Since this is also a key issue in the energy integration studies, a method has been developed in [61], and is used here, to calculate the said supply system in conjunction with a pinch analysis.

The heat cascade that is calculated in the process integration part, makes it possible to determine the Minimum Energy Requirements (MER) of the system. These represent the minimum amount of energy that needs to be externally supplied to the system. The satisfaction of the MER at minimum cost therefore depends on an optimal transformation of the available primary energy source (NG in this case) into useful energy to the processes (heat and power demands of the ship) [61]. As described in [61], this requires the definition of an optimal utility system with which the energy requirements are tied to their costs. Mixed integer linear programming (MILP) allows to model the heat cascade of the process and to obtain the cheapest utility system.

In this work, similarly to [3], the optimization problem is formulated as a MILP problem and solved with the OSMOSE framework. In OSMOSE, all technologies are modeled as described in Section 4.2, including all their corresponding streams, in order to define the heat cascade. Using this information and all the relevant restrictions, OSMOSE generates the appropriate MILP problem and solves it, yielding the optimal utility system configuration and operation.

The utilities and processes of the system involved in the MILP, and their respective streams, are identified in Section 4.4.1. A short version of the MILP formulation is next presented in Section 4.4.2, including some additional constraints that are particular to this problem.

4.4.1 Utilities, processes and their streams

Most of the components of the proposed energy system, mentioned in 4.1, are modeled as single utility units in OSMOSE. However, in the case of storage units, such as the batteries and the hydrogen storage, two separate units are defined for each of them: one that receives energy and one that transfers it. In the case of the SOFC,

also two independent units are defined, to represent its two operating modes. In addition, the total consumption of natural gas is modeled as an infinite source or utility that supplies all fuel demanded by the SOFC and the GT. Table 6 gathers all the utilities defined in OSMOSE and their respective streams.

Utility	**Streams**	
	In	**Out**
SOFC-Polygen-Power	CH_4	El, H_2, Ex, f
SOFC-Polygen-H2	CH_4	El, H_2, Ex, f
HT-PEMFC	H_2	El, Ex
Gas Turbine	CH_4	El, Ex
Hydrogen-Storage-In	H_2	-
Hydrogen-Storage-Out	-	H_2
Batteries-In	El	-
Batteries-Out	-	El
Gas Burner	CH_4	Ex
NG Supply	-	CH_4
Electric Motor	El	$Mech$
Electric Generator	$Mech$	El

Table 6: Sets of utilities and their corresponding streams defined in OSMOSE and involved in the resulting MILP formulation of the problem. Here El stands for electricity, $Mech$ for mechanical power, Ex for exhaust gases and f for fuel mix.

The heat and electricity demand of the cruise-ship are modelled as the two independent processes of the system. Both only have one stream defined, the heat stream (transferred with the hot water system) and the electrical power stream, respectively. As previously mentioned, these are the processes that must be supplied by the optimal utility system.

4.4.2 MILP formulation

The MILP problem, generated and solved in OSMOSE, is based on the formulation presented in [61]:

$$
\begin{aligned}
\text{minimize} \sum_{w=1}^{n_w} \quad & (C_{inv,w} y_w + C_{var,w} f_w) \\
\text{subject to} \sum_{w=1}^{n_w} \quad & f_w q_{ws} + \sum_{i=1}^{n} Q_{is} + R_{s+1} - R_s = 0, && \forall s = 1, ..., n_s \\
& f min_w y_w \leq f_w \leq f max_w y_w, && \forall w = 1, ..., n_s \\
& y_w \in \{0, 1\} \\
& R_s \geq 0, && \forall s = 1, ..., n_{s+1} \\
& R_s = 0, R_{ns+1} = 0
\end{aligned}
$$

Where n is the number of process streams for which the flowrate is considered constant; R_s the energy cascaded from the temperature interval s to the lower temperature intervals; Q_{is} the heat load of the process stream i in the temperature interval k (Q_a is >0 for hot streams and <0 for cold streams); n_w the number of utility streams; q_{wk} the heat load of the utility w in the temperature interval k for a given reference flowrate (q_{wk}>0 for a hot stream); f_w the multiplication factor of the reference flowrate of a utility w in the optimal situation; f_{min}, f_{max} the minimum and maximum values accepted for f_w; y_w the integer variable associated with the use of the utility stream w; $C_{inv,w}$ the fixed cost of using utility w; $C_{var,w}$ the proportional cost of using the utility w; and n_s the number of temperature intervals [61].

The assumptions made in [3], and in this work, are that the price of the natural gas c_{fuel} took a value of 0.5 USD/kg and the interest rate i a value of 0.05 [62]. Both considered fixed and size-dependent components of the technologies' investment costs are given in Table 7. In addition, the lifetime of conventional technologies is assigned to be of 20 years, while it varies from 5 to 8 for the newer ones. Based on an utilization of about 8000 h/year and operations of 50000 h, the lifetime of the SOFC systems is considered to be of 6 years. PEMFCs, on the other hand, are commonly expected to last for shorter periods than the SOFCs. In this case, however, since the PEMFC is not anticipated to run continuously in the given system configuration, a lifetime of 8 years is considered. This value is based on a use of 4000 h/year and on 30000 hours of operational life. It must be said that these considerations are rather conservative, given that a replacement of the whole system is necessary at the end of the lifetime. In reality, only the fuel stacks are replaced in this type of applications.

Components	**Source**	**Fixed inv. cost [kUSD]**	**Size-dependent inv. cost [kUSD/kW| kUSD/kWh*]**
SOFC-Polygen	[1]	12560	1.80
HT-PEMFC	[63]	0	3
Hydrogen Storage	[63]	0	0.045*
Batteries	[63]	0	1.08*
Gas Turbine	[64]	17280	1.23
Boiler	[64]	71	0.08

Table 7: Cost coefficients of the different utilities assumed in the original model. The asterisks indicate which of the values of the fourth column are measured in kUSD/kWh, instead of in kUSD/kW.

Additional constraints

To the formulation presented earlier, the following constraints, specific to this energy system, are added:

- Load change limitation. As mentioned in 4.2.5, the variation of load accepted by the SOFC is modeled with the following constraint:

$$P_{SOFC,t} - P_{SOFC,t+\Delta t} \leq \Delta P_{max,SOFC} \tag{2}$$

- Charging and discharging. For simplicity of the modeling, the energy storage units cannot be charged and discharged at the same time, leading to constraints of the following form:

$$\begin{aligned} y_{u1,t} + y_{u2,t} \leq 1, \qquad & \forall t \in \{1, N_t\}, \\ & u1 \in \{ES_{in}, HS_{in}\}, \\ & u2 \in \{ES_{out}, HS_{out}\} \end{aligned} \tag{3}$$

- Installation decision. The SOFC is assumed to always have the two modes of operation (baseline and hydrogen-overproduction) available. Therefore, the utilities that model the two modes cannot be decided to installed separately:

$$y_{SOFC_{power}} - y_{SOFC_{H_2}} = 0 \tag{4}$$

- Installed power. The installed power of both SOFC mode utilities must also be the same, as the make reference to the same technology:

$$f_{SOFC_{power}} - f_{SOFC_{H_2}} = 0 \tag{5}$$

- Mutually exclusive modes. Since the two operating modes of the SOFC cannot be used simultaneously, at any period of time t, a constraint of the following form is also added:

$$y_{SOFC_{power},t} - y_{SOFC_{H_2},t} \leq y_{SOFC,t}, \qquad \forall t \in \{1, N_t\} \qquad (6)$$

It is worth mentioning that the four last constraints are only necessary because of how the utilities have been modeled in OSMOSE. However, they do not have an important impact on the optimization, unlike the load change limitation constraint of the SOFC.

5 Results on the optimization of the nominal system

The optimal energy system design obtained in Baldi's work, as well as the main characteristics of its optimal operation, are presented in this section. The idea is to give some perspective on the orders of magnitude of the various outputs, such as the costs of the components, and the optimal distribution of their installed power and power generation, in the nominal case (with the input parameters taking their nominal values). These results serve to see how the proposed system is optimally operated in the base case and will later help to understand how this operation adapts to the different modifications performed on the input parameters, as described in Section 7.

An important result of his work, is the confirmation of the benefits, in both efficiency and economic terms, of using a SOFC-PEMFC hybrid system. According to [3], an energy efficiency of 72.9% can be reached with the hybrid system, while only a 70.0% can be attained when the PEMFC is excluded. This increase in overall efficiency is also translated into a decrease in operating costs. This outcome justifies the incorporation of the latter fuel cell in the current work.

The resulting installed power of all components and their corresponding investment costs, in the hybrid case, are given in Table 8. Figure 4 depicts, on the other hand, the distribution of power and heat generation, and fuel consumption, among the different technologies. It is shown that the SOFC supplies most of the ship's annual energy demand: 75.5% of its power demand and 90% of its heat demand, in the hybrid case. The contribution of the PEMFC is still considerable, however, as it covers 14.2% of the power demand. The battery fulfills 9.5%, while the remaining 0.8% is generated by the GT. Despite the large installed power of the GT, its share of covered power demand is very low as it only operates in marginal periods, such as when the ship sails in high-speed mode (only in extreme days). As in those periods the peak power demand can become 5 times the mean demand, a GT of over 30000kW needs to be installed, representing the largest share of the investment cost,

as indicated in Table 8. With respect to the heat demand, it is very rarely supplied by the boiler, causing its contribution (of 5.9%) to be rather marginal.

Technology	**Installed E. Power (kW/kWh*)**	**Installed Th. Power (kW)**	**Tot. Inv. Cost (k$)**
SOFC-Polygen	4675	1900	1766
HT-PEMFC	1660	385	710
Hydrogen Storage	310E6*	-	56
Electric Storage	360E6*	-	2560
Gas Turbine	18570	33760	2980
Boiler	-	990	72

Table 8: Results on the installed power of the different technologies and their respective total investment costs, when the nominal input data are used.

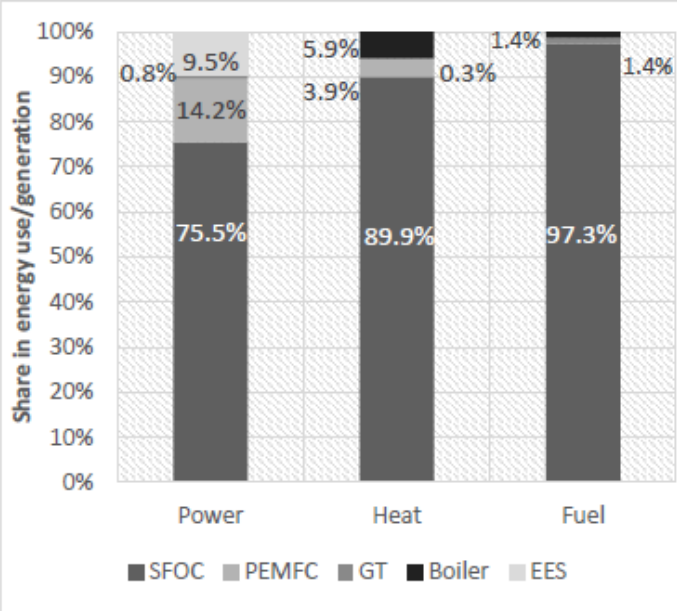

Figure 4: Yearly heat and power generation distributions among the different utilities, as well as their share of fuel consumption. [3]

Finally, Table 9 shows the optimal total cost obtained under this scenario, including as well the values of its two components: the investment and operating costs. As observed, the operating cost of the energy system represents the largest share (80%) of the total cost.

Total Cost(M$)	**Investment cost (M$)**	**Operating cost (M$)**
43.6	8.1	35.5

Table 9: Total cost of the optimal energy system design, with the corresponding shares of investment and operating costs.

Chapter 3: Uncertainty Characterization

6 Uncertainty Characterization

The first step in any study involving uncertainty is to define the uncertainty of the input parameters, to quantify it. In other words, the input factors of the problem need to be assigned with a quantitative measure of their uncertainty. Once these values have been determined, a proper study of their impact can be carried out. In this project, this is achieved by means of Sensitivity Analysis, with the results from this characterization being its most important input information [65].

There are several approaches that can be followed to characterize uncertainty. Some authors, like Dubuis [54] propose the use of Probability Distribution Functions (PDFs) when accouting for uncertainty in energy systems design. However, as stated by Dubuis, enough information can often lack for the definition of the distribution parameters. Siddiqui and Marnay [66] have also argued that reliable empirical basis are frequently absent when PDFs are considered in stochastic models. In other cases, simpler definitions of uncertainty are assumed, such as constant percentages of variation assigned uniformly to the group of parameters considered as uncertain. Different levels of uncertainty can also be applied, as has been done in [67] , where cost parameters were given either a low (10%), a medium (30%) or a high (50%) uncertainty value, depending on the complexity and maturity of the technologies.

However, as noted by Moret [15], most of the time only a small and arbitrarily-selected subset of parameters are considered as uncertain. These are usually related to costs or efficiencies in energy systems design. In addition, the characterization of uncertainty often represents a marginal study, that is carried out to be the input of other, more meaningful analysis.

In this work, the interest behind the uncertainty characterization is not only to obtain an input necessary for the sensitivity analysis. The idea is also to contribute in the subject and provide information that could be used in other studies involving uncertainty. In other words, the results on the current technologies' uncertainty, which will be given in relative terms, could be incorporated in any related future study. Further, the aim is also to include all input parameters in the characterization, to avoid the risk of misleadingly assuming that some factors are certain.

An adapted version of the characterization method proposed by Moret is applied to the present model. As detailed in Section 6.1.1, the approach is based on the definition of ranges of variation, for all the uncertain parameters, depending on a set of criteria. These ranges are suitable not only for sensitivity analysis, but even for robust optimization problems, which is a possible continuation to this project.

The application of the method to the current case study is presented in Section

6.2. Finally, the corresponding results are provided in Section 6.3, and subsequently analyzed in Section 6.4.

6.1 Method

The uncertainty characterization method, based on Moret's work [15] and followed in this project, is summarized in Figure 5. After having identified all input parameters of the model, these are preliminarily screened and grouped, as will be detailed next. The remaining factors are considered as uncertain and five different criteria are applied to each of them. Each of the criteria represents a distinct approach to evaluating the uncertainty of a given parameter. It is possible for a factor to have more than one applicable criterion.

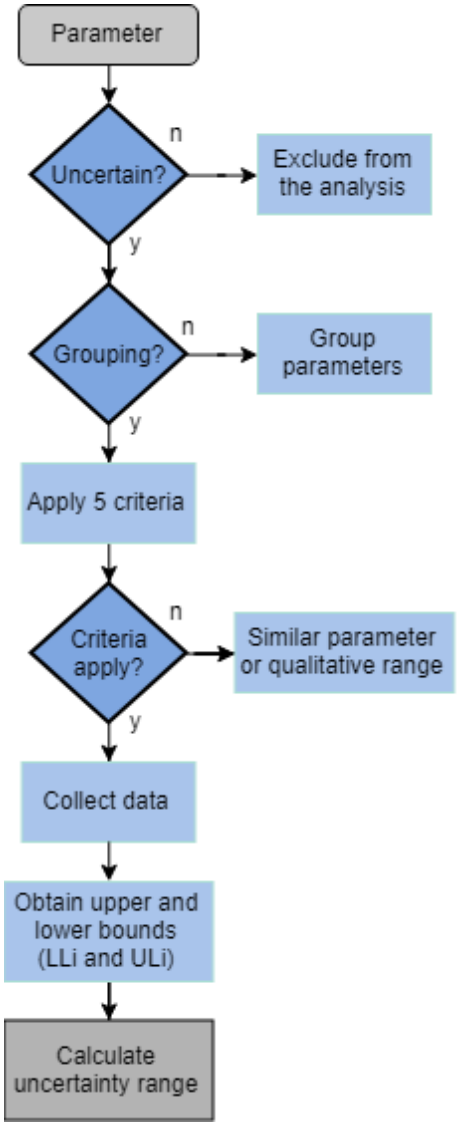

Figure 5: Flow chart representing the uncertainty characterization method followed in this project. Built based on [].

For each applicable criterion, the corresponding required information is gathered. The collected data allows to determine the upper and lower bounds for each input factor, UL_i and LL_i, respectively. These terms correspond to the highest and lowest values found or computed (depending on the criterion), of the parameter. Using these and the nominal values of each factor, its uncertainty range is finally computed. The complete process therefore consists of:

1. **Identification and listing of all input parameters**
   All input parameters are first gathered and listed, to avoid arbitrarily excluding some of them from the study.

2. **Preliminary screening and grouping**
   The parameters that are known to be completely certain or that have no influence on the outputs are disregarded in an initial screening. This is the case, for example, of the number of periods or time steps over which a model is analyzed, or of the material properties that are considered in it. Next, the remaining parameters are grouped into different categories to simplify their characterization. The grouping is done based on similarities between them, assuming that the parameters belonging to a given category bear similar uncertainty. In this way, it is only necessary to tipify the uncertainty of a representative parameter of each category. The resulting uncertainty range of the representative factor, expressed in relative terms, is subsequently applied to all the other parameters belonging to its group.

3. **Application of uncertainty characterization criteria**
   There are various criteria that can be helpful for characterizing the uncertainty of a parameter. As previously mentioned, they represent different techniques for defining this uncertainty. The five considered criteria are: *C1: a) Can the uncertain parameter be modeled? If yes, b) is the developed model incorporated into the primary model?; C2: Is there a range that has already been proposed in the literature? ; C3: a) Can a range be obtained from existing forecasts? b) Is there available information about the accuracy of past forecasts; C4: Can (historical) data be used?; C5: Does the parameter depend on the Decision Maker (DM)? Are there available expert opinions (EOs)? If it depends on the DM, b) is it only their choice?*
   For each parameter, the information relative to each applicable criteria is gathered.

4. **Calculation of uncertainty range**
   The maximum and minimum values of all representative parameters are determined. These values are obtained or calculated depending on the criteria that has been applied. For a given parameter i:

- If C1 applies and the model is external: UL_i and LL_i are obtained from external model
- If C2 applies: UL_i and LL_i are extracted from the literature
- If C3 applies: UL_i and LL_i are extracted from a forecast. If possible, the corresponding errors are also collected
- If C4 applies: UL_i and LL_i are obtained from the available data
- If C5 applies and it does not depend only on the DM's choice: UL_i and LL_i are obtained based on information or on an opinion. If it only depends on the DM's choice: parameter i is not uncertain or is a decision variable.

Finally, the uncertainty associated to a given parameter i is calculated, provided its corresponding values UL_i and LL_i, and its nominal value, $X_{0,i}$. Its uncertainty is computed as the largest percentage difference between these bounds and the model's original value, as indicated in (7).

$$\text{Uncertainty}_i = \max\{\frac{UL_i - X_{0,i}}{X_{0,i}}, \frac{X_{0,i} - LL_i}{X_{0,i}}\} \tag{7}$$

The resulting percentages of uncertainty are applied to the corresponding other members of each category, generating conservative symmetrical ranges of uncertainty. These final ranges will serve as inputs for the second part of the project: the Sensitivity Analysis.

6.1.1 Uncertainty characterization criteria

The five criteria for characterizing uncertainty involved in the method proposed by Moret are described as follows. They are applied in parallel to all the uncertain inputs [15]:

C1 *a) Can the uncertain parameter be modeled? If yes, b) is the developed model incorporated into the primary model?*
For some uncertain parameters it may be possible to find an already existing model or to develop it. The uncertain parameter (θ) is mathematically defined as a relation where $\theta = h'(\theta'_1, ..., \theta'_k)$, in which $\theta'_1, ..., \theta'_k$ are the k parameters of h'. Thus, $\theta'_1, ..., \theta'_k$ become the new uncertain parameters under study. The model can be incorporated into the main one, meaning it would be an internal paramater model. Otherwise, if it is too complex, it is not integrated and remains external to the main model. This decision is taken by the modeler.

C2 *Is there a range that has already been proposed in the literature?*
By doing a review of the related literature, it can be found that the uncertainty of the concerned parameter has already been evaluated. A proposed range or PDF is available.

C3 *a) Can a range be obtained from existing forecasts? b) Is there available information about the accuracy of past forecasts*
The future values of some parameters may have already been forecasted and are available to the modeler. In some cases, forecasts can even also provide uncertainty ranges for the suggested nominal values. Another option is to define such range based on various forecasts. Furthermore, the accuracy of the consulted forecasts may be roughly assessed, if information about the precision of earlier ones is available.

C4 *Can (historical) data be used?*
Available data, either current or historical, can be used to obtain the parameter's range of uncertainty. It is thus assumed that future variations can be represented by current or past ones.

C5 *Does the parameter depend on the Decision Maker (DM)? Are there available expert opinions (EOs)? If it depends on the DM, b) is it only their choice?*
The uncertainty of some parameters could be influenced by the DM. For instance, if the DM is the government, a policy could be implemented, and any information available about this policy should be considered for defining the ranges. It can also happen that the parameter only depends on the DM and its value can be known. In such case, the factor in question can be deleted from the list or alternatively be introduced as a decision variable.

6.2 Application to the case study

The method described in Section 6.1.1 is applied to the model of the cruise-ship energy system. The corresponding input parameters are identified and initially screened, and grouped. The applicable criteria are subsequently identified and pertinent information is collected. Nonetheless, due to time limitations and technical complications some simplifications were made:

- For each uncertain parameter, all the applicable criteria were identified. However, as will be later detailed, only a few of them were applied in some cases. The alternative, unused characterization approaches were either considered tedious or rather inaccesible. An example is the consulting of EOs.
- In other cases, it was not possible to find pertinent information and simplified uncertainty ranges were assigned. These cases are identified in Section 6.3.
- Although it was not originally intended, a few uncertain parameters ended up being excluded from the whole analysis. This was mostly due to technical complications with the model. The factors in question are indicated in Section 6.3.

These simplifications, however, remain as a part of the possible future work. Including absolutely all uncertain parameters to the study, for the reasons previously mentioned, would a very high interest.

6.3 Results

Listing of input parameters

A set of 208 parameters is initially identified as the inputs to the model of the cruise-ship energy system. Table 10 summarizes the different types of parameters that are collected, with the number of factors that are under those names. A small description of what they represent is also included.

Preliminary screening

A screening prior to the uncertainty characterization is performed. The objective is to discard all the parameters that are known to be certain. If there is any doubt, the input is assumed to be uncertain. Parameters that have no real meaning or an impact on the objective function are also removed. As mentioned in the previous section, some uncertain inputs are excluded from the analysis for computational and time limitations. These, however, bear important uncertainty and should be included in any future investigation.

The parameters that are removed from the study are listed next, including an explanation to why they are removed:

- f_{min}**(Tech),** f_{max}**(Tech),** P_{max}**(Tech),** Q_{max}**(GB)**:
  The multiplication factors' bounds f_{min}(Tech), f_{max} and the maximum power values of the utilities act together in the objective function. In this problem, however, they do not have a real meaning. It is assumed that all technologies can grow linearly and have no limit in their size. The values for their maximum electrical and thermal powers are simply chosen large enough for them not to interfere with the optimization process.
  This corresponds to an exclusion of 18 parameters.

- L_{min}**(Tech)** $\forall$**Tech**$\notin$**{SOFC, GT}**:
  These parameters are defined by default and to a null value. Technologies except for the SOFC and the GT are assumed to not have minimum loads. This represents the removal of 4 parameters.

Parameter type	**Units**	**N° of parameters**	**Description**
f_{min}(Tech)[a]	[-]	6	Minimum multiplication factor
f_{max}(Tech)[a]	[-]	6	Maximum multiplication factor
L_{min}(Tech) [a]	[-]	6	Minimum load
L_{max}(Tech)[a]	[-]	6	Maximum load
$C_{inv,fix}$(Tech)[a]	[k$]	6	Fixed component of investment cost
$C_{inv,var}$(Tech)[a]	[k$/kW, k$/kWh]	6	Size-dependent component of investment cost
$C_{op,NG}$	[$/kg]	1	Natural gas price
P_{max}(Tech)[b]	[kW]	5	Maximum electrical power
Q_{max}(GB)	[kW]	1	Maximum thermal power
$Charge_{max}$ (ES)	[kWh]	1	Maximum charge accepted by batteries
LHV_{H_2}	[kJ/kg]	1	Hydrogen's Lower Heating Value
T_{in}(Stream)[c]	[°C]	9	Inlet temperature
T_{out}(Stream)[c]	[°C]	9	Outlet temperature
η_{el}(Tech)[d]	[-]	4	Electrical efficiencies
η_{th}(Tech)[e]	[-]	3	Thermal efficiencies
η_{mec}(HS)	[-]	1	Mechanical efficiencies
η_{dis}, η_{ch}(ES)	[-]	1/1	Charging and discharging efficiencies (Battery)
ΔP_{max}(SOFC)	[kW]	1	Maximum variation of load
H^i_{ref} (SOFC)	[kW]	2	Reference enthalpies of SOFC streams (f and ex)
$P^j_{max,ref}$ (SOFC)	[kW]	2	Reference max power of SOFC op. modes
$NG_{in,ref}$(SOFC)	[kW]	1	Reference fuel consumption
$H2_{out,ref}$(SOFC)	[kW]	1	Reference Hydrogen production
$Demand_{El}$(t)	[kW]	48	Total electrical power demand at each time step t
$Demand_{heat}$(t)	[kW]	48	Total heat demand at each time step t
Lifetime(Tech)[a]	[y]	6	Technology lifetime
Occ (Typ. day)	[d/y]	4	Occurrence of a given typical day
t_{op}(period)	[h]	12	Operation time of a given period (12 periods/day in total)
n_{op}	[y]	1	Number of years of operation under study
i	[-]	1	Real discount rate
Total		201	

Table 10: Summary of input parameter types of the cruise-ship energy system model. [a] Tech∈ {SOFC, PEMFC, HS, ES, GB, GT}, [b] Tech∈ {SOFC, PEMFC, HS, ES, GT}, [d] Tech∈ { PEMFC, ES, GT, EG}, [e] Tech∈ { PEMFC, GB, GT}

- LHV_{H_2} **and** n_{op} :
  Material properties, such as the LHV of hydrogen, are considered to be certain. On the other hand, the number of periods of operation under which the ship is optimized is also considered as fixed. The energy system is studied for the same duration as in Baldi's work. These 2 parameters are therefore discarded.

- **Occ (Typ. day) and** t_{op}**(period)**:
  These two parameters are strongly related to the modelling of the electrical and heat demands of the ship. The first one indicates how many days in a year, one of the four modelled typical days occurs. The second the duration of the time steps in which one day is divided. Although clearly uncertain, the characterization of Occ (Typ. day) and t_{op}(period) is rather complex. The uncertainty of the energy demand is therefore modelled through $Demand_{El}$(t) $Demand_{heat}$(t).
  This corresponds to the removal of 16 parameters.

- T_{in}**(Stream),** T_{out}**(Stream) and** i:
  The input and output temperatures of the utilities' streams are considered uncertain, as well as the interest rate. However, their inclusion in the problem was prevented due to technical issues. The changes in the temperatures caused problems with feasibility and the execution of the model. In addition, the automatic modification of the interest rate inside the model was not trivial.
  This supposes the exclusion of 19 parameters from the study.

After the screening, a total of 142 input factors remain, all of which the uncertainty is to be characterized.

Grouping

The uncertain parameters are grouped to form categories. This is done based on the similarities between them and then choosing a representative parameter for each group. The resulting groups and their corresponding representative parameters are included in Table 12.

In this case, some of the utility-related factors are classified depending on the maturity of the technologies. The distinction is made between the more mature, well-established technologies and those that are new, and still not produced in large scales. Only the fuel cells (PEMFC and SOFC) are considered to belong in the latter class. This grouping is applied to parameters that are common to all utilities, such as investment costs or efficiencies (distinguished by their kind). However, no distinction is made in the uncertainty of the utilities' lifetimes, following the suggestions in [15]. Their lifetimes are, therefore, similarly characterized.

Uncertainty characterization and range calculation

The characterization criteria is applied to the representative parameters of each group. Pertinent information is gathered and the uncertainty ranges are finally calculated as indicated in (7). In a few cases, however, a simplified characterization is performed. Further details on this step are provided next, in function of the parameter categories:

- Load bounds
  The uncertainty of the utilities' load bounds, L_{min} and L_{max}, is characterized in a simplified manner. A percentage of variation of 20% is assigned to all the parameters under this category. In the cases where the L_{max} has a nominal value of 1, the range is not centered around it. Instead, the range is defined under it, i.e [0.8, 1].

- Investment costs
  Both components of the utilities' investment costs, $C_{inv,var}$ and $C_{inv,fix}$, are characterized depending on the maturity of the utility.
  For the costs of newer technologies, under the category $C_{inv,new}$, $C_{inv,var}$ (SOFC) is chosen as the representative parameter. For this factor, it is possible to apply criteria C3a, in the form of forecasts or estimations about the cost of mass producing this fuel cell. In addition, thermo-economical studies concerning the use of SOFCs, that provide their cost estimations, are also consulted. An upper bound $UL($ $C_{inv,var}$ (SOFC)) of 2.6 k\$/kW and a lower bound $LL($ $C_{inv,var}$ (SOFC)) of 1.1 \$/kW are finally obtained. Using (7), it leads to an uncertainty range of ±45%.

  A similar procedure is followed for the mature technologies, of which the representative parameter is $C_{inv,var}$ (GT). In this case, only data from previous studies are consulted. Only values lower than the nominal are found, obtaining a $LL($ $C_{inv,var}$ (GT)) of 0.865 k\$/kW [68]. The resulting uncertainty range therefore corresponds to a ± 30%.

  As the nominal values of $C_{inv,fix}$ of some utilities are 0, a different uncertainty definition is used to account for the effect of adding a fixed component to the investment cost of these technologies (PEMFC, HS and ES). These parameters are assigned with a maximum value equal to what the corresponding variable investment cost would be if the final multiplication factor was 0.1. This is mathematically expressed in (8).

$$\max(C_{inv,fix}) = 0.1 \cdot C_{inv,var} \cdot P_{max} \tag{8}$$

- Gas Price
  For the gas price, denoted as $C_{op,NG}$, both forecasts and historical data are

reviewed. Forecasts seem to agree in the expectation of smaller variations in the NG price for the next 10 years compared to those experienced in the past 4 years. An increase of only 7 %by 2022 is forecasted by Comesa [69]. However, variations of up to 50% have been seen in the last 4 years [69] [70]. As part of the conservative approach of this project, the final NG price range is based on the historical data.

- Efficiencies
  For the newer technologies, all efficiency types are similarly characterized, as the available data are more reduced. However, the distinction between thermal, electrical or storage-related efficiencies is made for the mature utilities. Furthermore, in all cases only the criterion C4 is applied, basing the characterization in current available data. The summary of the collected data and the resulting uncertainty ranges is provided in Table 11.

Category	**Representative**	LL_i	UL_i	**Uncertainty range**
$\eta_{th,mature}$	η_{th}(GB)	0.8	0.98	[-15%,15%]
$\eta_{sto,mature}$	η_{dis}(ES)	0.99	0.94	[-5%,5%]
$\eta_{el,mature}$	η_{el}(GT)	0.29	0.4	[-12%,12%]
η_{new}	η_{el}(PEMFC)	0.35	0.7	[-35%,35%]

Table 11: Summary of the uncertainty range calculation for the parameters relative to efficiencies.

- Energy demands
  The parameters D_{El}(t) and D_{heat}(t) represent the total energy demands at a given time step of each typical day. As there are 4 typical days, of 12 different time steps each, there is a total of 48 uncertain parameter values for both the electrical and the heat demand. Instead of characterizing each of these, the idea is to only measure the uncertainty involved in the mean demand values and the deviations from those mean values in all time steps. Expressed mathematically, these respectively correspond to $D_{m,i} = \sum_{t=1}^{N_t} \frac{D_i(t)}{N_t}$ and $\Delta D_i(t) = D_i(t) - D_{m,i}$, $\forall t \in \{1, ..., N_t\}$, where $i \in$ {El, Heat}.

  For a given demand type i, $D_{m,i}$ is assigned with an uncertainty, modelled with the new parameter $C_m(i)$. All the 48 values of $\Delta D_i(t)$ are given the same percentage of variation, denoted as $C_\delta(i)$. This means that, in a given scenario of uncertainty, the mean demand value will differ in $C_m(i)$ from its nominal value, and the deviation of $D_i(t)$ w.r.t to its mean value will differ in $C_\delta(i)$ from the nominal deviation $\forall t \in \{1, ..., N_t\}$.

Therefore, it could be said that the original demand parameters are modelled as expressed in (9), where $C_m(i)$ and $C_\delta(i)$ are the new uncertain parameters.

$$D_i(t) = D_{m,i} \cdot C_m(i) + \Delta D_i(t) \cdot C_\delta(i) \ldots \forall t \in \{1, ..., N_t\}, i \in \{\text{El, Heat}\}, \quad (9)$$

$C_m(i)$ and $C_\delta(i)$ having a nominal value of 1, they are assigned with a range of uncertainty of ± 10%.

- Utilities' lifetime
  Based on the work of [15], the lifetime of all utilities is characterized with the same relative level of uncertainty. Here, the gas boilers' lifetime is also chosen as the representative parameter. Therefore, it is possible to use the relative range of variation provided in such work. In round numbers, this corresponds to an uncertainty of ±25%.

Table 12 summarizes the results of the uncertainty characterization. The applied criteria, the resulting ranges of variation and the most relevant consulted sources are included.

Category	**Representative**	**Applicable criteria**	**Uncertainty Range**	**Source**
L_{min},L_{max}	-	-	20%	-
$C_{inv,mature}$	$C_{inv,var}$(GT)	C4	[-30%,30%]	[68]
$C_{inv,new}$	$C_{inv,var}$(SOFC)	C4, C3a	[-45%, 45%]	[71]
$C_{op,NG}$	-	C4, C3b	[-50%,50%]	[70]
$\eta_{th,mature}$	η_{th}(GB)	C4	[-20%,20%]	[72]
$\eta_{sto,mature}$	η_{sto}(ES)	C4	[-5%,5%]	[73]
$\eta_{el,mature}$	η_{el}(GT)	C4	[-12%,12%]	[74]
η_{new}	η_{el}(PEMFC)	C4	[-35%,35%]	[75] [76] [77]
ΔP_{max}(SOFC)	-	-	[225kW, 1500kW]	-
C_m,C_δ	-	C1a*	[-10%,10%]	-
Lifetime(Tech)	Lifetime(GB)	C2	[-25%,25%]	[15]

Table 12: Summary of the uncertainty characterization results. The provided sources are the most relevant consulted ones.

6.4 Discussion

From the performed uncertainty characterization, it results that the gas price is the input parameter with the widest range of variation. This is largely due to the fact that this fuel's value has significantly fluctuated in recent years. However, if the measure of uncertainty of this factor only relied on available forecasts, the resulting range would be considerably smaller. Nonetheless, by accounting for their accuracy, based on past forecasts, the results of both approaches do not differ as greatly.

The level of uncertainty of this input is followed by that of the parameters relative to non-mature technologies. These include the investment costs and the efficiencies of this type of utilites. It is found, however, that the data available for characterizing these parameters' uncertainty is considerably more reduced than for those of the more mature technologies. This is influenced by the fact that these fuel cells are still not well established in the market, that they are rather in an investigation stage and being produced in small scales. Nonetheless, there are several studies that have been or are being carried out, including economic evaluations, and allowing to estimate the costs of these technologies. In addition, governmental institutions, such as the DOE of the US, have also set future target costs for these fuel cells. This gives an idea of the costs that are expected for when the FCs are finally produced in mass.

It is also interesting to see that, even for parameters associated to the more mature technologies, their uncertainty is not negligible. This is particularly true for the uncertainty linked to the investment costs of components such as the gas turbine or, in less measure, the gas boiler. Even though they are well established technologies, that have been in the market for many years, the cost values found in the literature show noticeable divergence. This only enhances the idea of newer equipments necessarily having an even more substantial uncertainty.

It is equally important to say that the characterization of some factors relative ended up being rather arbitrary. This is the case of parameters relative to the load limitations or to the energy demands. This is mostly due to time and resource limitations. The considered ranges have allowed to assess, in the sensitivity analysis, the importance of uncertainty being associated to these parameters. However, these uncertainty values should not be taken as a well founded reference for future studies.

Finally, it is essential to differentiate the parameters that were initially excluded from the study for being certain or meaningless from those that are uncertain and were excluded for simplification. These are distinguished in Section 6.3. Those that were removed, only for technical or time limitations, should be considered in any relative future study. In any sensitivity analysis, arbitrary exclusions of parameters should be avoided as much as possible.

Chapter 4: Sensitivity Analysis

7 Sensitivity Analysis

As revealed in Section 6.3, the uncertainty involved in the inputs of the present model is, at first sight, significant, as the uncertainty ranges take values that reach up to $\pm$ 50%. However, the only way to measure its actual relevance is by assessing its impact on the results. There could be large possibilities of variation in the inputs and yet have no importance. The interest now is, therefore, to judge if the presence of these uncertainties have a meaningful influence on the model's outputs, and ultimately, on the optimality of the proposed energy system. One way to achieve this is by means of Sensitivity Analysis.

In general terms, Sensitivity Analysis consists of the investigation of how the different uncertainty sources found in the inputs of a mathematical model correlate with the uncertainty in the outputs [5]. The information gathered can, not only help understading the input-output relationships, but can also serve to detect errors inside the model if the resulting correlations are counter-intuitive. In a way, the analysis can contribute to the validation or evaluation of a model's capacity to emulate reality, which is one of the objectives of this work.

By identifying the most impactful sources of uncertainty, Sensitivity Analysis can help reduce this uncertainty and improve the quality of the model. Once pintpointed, larger and deeper focus can then be made on the modelling or characterization of particular inputs, knowing that the time invested will be fruitful. Finally, this type of study can also serve, in the presence of uncertainty, to evaluate the robustness of the model's results [65]. In other words, to assess the impact of uncertainty on the outputs, which is the main goal of the present project.

Most sensitivity analysis techniques found in the literature are based on derivatives [5]. The partial derivative of the output Y_j, of a model, with respect to an input factor X_i is taken as a measure of the sensitivity of Y_j versus X_i. As this derivative is necessarily computed at a fixed point in the input space, these are considered to be Local Sensitivity Analysis (LSA) methods [65]. Although the derivative-based approach has the advantage of being very computationally efficient, they have a major limitation for when the linearity of the model is unknown or its inputs are uncertain. The information derivatives provide is only relevant to the base point in which they are computed, thus leaving the rest of the input space unexplored [5]. Given that the model involved in this work is not globally linear, hence restricting the use of linear extrapolation, this restraint to local methods should not be ignored.

With variance-based methods, the sensitivity is measured by the amount of variance produced in an output by a given input. These, in contrast to local methods, allow to analyze the whole input space, identifying interactions between inputs and nonlinear

responses [65]. For this reason, variance-based techniques are considered to study sensitivity globally rather than locally: GSA (Global Sensitivity Analysis) vs LSA. However, their computational cost can be very high, especially if the model involved is also heavy or if it has an important number of input parameters, which is the case.

The Elementary Effects (EEs) method manages to find a good compromise between local and global techniques. Despite its reliance on the concept of variation about a base point and its one-at-a-time (OAT) sampling approach, it attempts to overcome the biggest disadvantage of derivative-based methods. The idea behind this method is the elimination of the base-point dependence by allowing inputs to vary within larger ranges and finally average the ensemble of local sensitivity values. As a result, the EEs manages to cope with computationally costly models, giving insightful results even when a reduced (yet well distributed) set of sample points are considered [78].

In present sensitivity analysis, the EEs method is applied to the model of the cruise-ship energy system, as is described next. First, a more detailed description of the method is given in Section 7.1, including the sampling strategy that is used and the corresponding computation of sensitivity measures. This is followed by an explanation of how the method is applied to the case study in Section 7.2, where the numerical implementation, and the two analysis to be performed are also detailed. The results of both studies, as well as their discussions are finally presented in Section 7.3 and Section 7.4, respectively.

7.1 The Elementary Effects Method

The elementary effects method is an effective way of screening the input parameters of a model for their relevance to the outputs of interest. As it name indicates, it is based on the concept of elementary effects, which was first suggested by Morris in 1991. To define this, first consider a model with k independent inputs X_i, $i = 1, ..., k$, the input space created by which is discretized into a grid Ω of p selected levels. Then, the elementary effect of the i-ith input parameter, for a given value of $\boldsymbol{X}$, is defined as

$$EE_i = \frac{Y(X_1, X_2, ..., X_{i-1}, X_i + \Delta, ..., X_k) - Y(X_1, X_2, ..., X_k)}{\Delta}, \tag{10}$$

where p is the number of levels, Δ corresponds to a value inside $\{\frac{1}{p-1}, ..., 1 - \frac{1}{p-1}\}$, $\boldsymbol{X} = (X_1, X_2, ..., X_k)$ is any chosen array of values in Ω such that the perturbed point $(\boldsymbol{X} + e_i\Delta)$ is still contained in Ω for each index $i = 1, ..., k$, and e_i is a vector of zeros except for the unit of its i-th component.

By sampling randomly different values of $\boldsymbol{X}$ out of Ω, it is possible to generate the distribution of elementary effects of a given input i. This distribution is denoted

as F_i, hence $EE_i \sim F_i$. As F_i is a finite distribution, its number of elementary effect values can be determined and is a function of p, k and Δ.

To give a clearer idea on how the different values of EE_i are computed, consider the case of $k = 2$, $p = 4$ and $\Delta = 2/3$. Figure 6 shows the corresponding two-dimensional input space, where both parameters take four different values ($p = 4$) inside Ω. Each arrow indicates one computation of EE_1 (when X_1 is varied), that is performed between two values of X_1 separated a distance of Δ. In this case, the number of total elementary effects associated to X_i is eight (8 arrows).

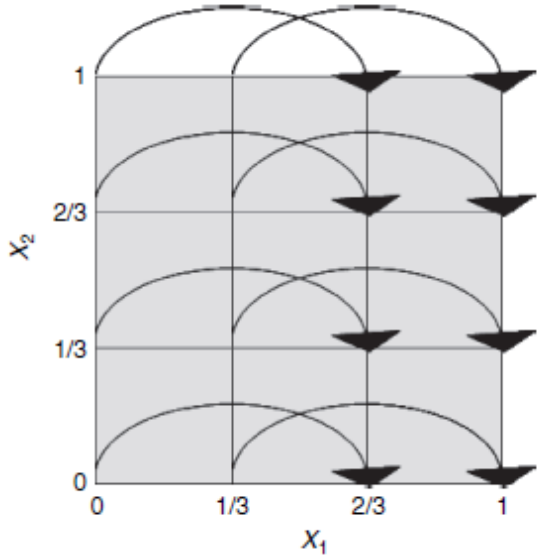

Figure 6: Representation of example of a four-level grid ($p = 4$) in a two-dimensional input space ($k = 2$), where Δ takes the value of $2/3$. The arrows identify the eight perturbations needed to estimate all the elementary effects associated to input X_i

The two measures of sensitivity suggested by Morris correspond to the estimates of the mean and of the standard deviation of the distribution F_i, denoted by μ and σ, respectively. The value of μ quantifies, in a qualitative manner, the overall impact of the input parameter i on the output of interest. The standard deviation, on the other hand, assesses the variation in the effects of the factor i, due to nonlinearities and/or to interaction with other parameters. If the value of σ is high, then there is a large variation in the values of EE_i, indicating that the choice of sample points is strongly influential and hence, so are the values of the other factors. In the opposite case, of σ being low, the other parameters have very little influence on the effect of X_i.

Another interesting distribution can be defined by gathering the absolute values of the elementary effects, it being denoted as G_i, and thus, $|EE_i| \sim G_i$. If, rather

than μ, the mean's estimate of G, μ^*, is used to measure sensitivity, the risk of making type II errors (deeming as non-influential factors that are actually influential) is eliminated. However, if F_i contains both positive and negative values, it is very possible to commit type II errors when computing μ. Some cancelations can occur and important parameters can end up receiving small values of μ. Although this issue can be mitigated if both the values of μ and σ of all input factors are considered in the analysis, the use of μ^* has more benefits. It is a more concrete and efficient measure, especially in cases where there are multiple outputs of interest. Plus, the value of μ^* has been proved to give a good approximation of the total sensitivity index S_T, an index that serves to single out the non-influential factors [5].

Although the relevance for this project of the values obtained for μ^* is larger, both mean estimates are computed and considered. The values of μ^*, with respect to all the outputs of interest, will be used to rank the input factors in function of their influence on the outputs. On the other hand, the values of μ with respect to some outputs will be studied, to confirm that the sign of the relationships between the inputs and the outputs are reasonable. This will therefore serve to verify that there are no major mistakes involved in the modelling of the energy system.

The sampling method followed to compute the estimates of the three sensitivity measures (μ, σ, μ^*) is described next in Section 7.1.1. Finally, the calculation of the values of these statitistics, once the model is ran for all the generated sampling points is detailed in Section 7.1.2.

7.1.1 The sampling strategy

Given a simple definition of the inputs' uncertainties, such as the ranges calculated in the previously presented uncertainty characterization section, the Morris method generates a discrete sampling of these parameters. In this sampling, r trajectories are defined, in each of which all input parameters are made vary once, producing a total of $k + 1$ different steps. In other words, $(k + 1)$ points of the input space are visited in each trajectory, yielding a total of k elementary effects (one for each input factor). This entails the generation of a total of $r(k + 1)$ sample points, each representing a run of the energy system's optimization model.

In order to produce the trajectories, the next steps are followed, as described in []:

1. Choose a random base value $\boldsymbol{x}^*$ for the vector of input factors $\boldsymbol{X}$ out of the $p-$level grid Ω. This base value, while not belonging to any trajectory, serves to generate all sample points by perturbing one or more of its components.

2. Generate the first trajectory point $\boldsymbol{x}^{(1)}$ by increasing one or more of the components of $\boldsymbol{x}^*$ by a quantity of Δ and making sure $\boldsymbol{x}^{(1)}$ still belongs to Ω.

3. Compute $\boldsymbol{x}^{(2)}$, the second trajectory point, based on $\boldsymbol{x}^*$ and ensuring that its i-th component is different from that of $\boldsymbol{x}^{(1)}$, as shown in (11). Pick out the index i randomly from the set $\{1, 2, ..., k\}$.

$$\boldsymbol{x}^{(2)} = \boldsymbol{x}^{(1)} \pm e_i \Delta \tag{11}$$

4. The third point, $\boldsymbol{x}^{(3)}$, is generated similarly to $\boldsymbol{x}^{(2)}$ but both differing in only one component j, with $j \neq i$.

5. Continue the sequence until obtaining $\boldsymbol{x}^{(k+1)}$ and finally closing the trajectory.

This procedure is illustrated in Figure 7, in an example of a tridimensional input space ($k = 3$).

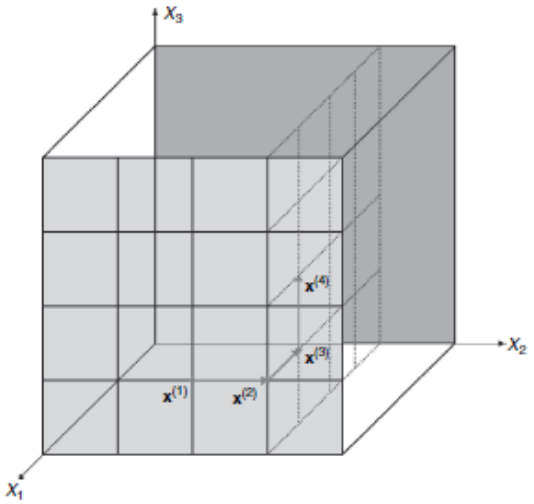

Figure 7: Example of how a trajectory can be built in a model's input space, for when $k = 3$. Extracted from [5]

Since in all the steps of the different trajectories, where a given parameter is varied, all the other parameters are taking different values across trajectories, it is still possible to account for the interaction between the input parameters. This is, in fact, why this method is considered to be halfway between local and global methods.

7.1.2 Sensitivity measures computation

As previously mentioned, the model is ran $(k + 1)$ times for each trajectory that is built, therefore leading to a total of $r(k + 1)$ model executions. Each of these runs makes it possible to compute the elementary effects that correspond to all k input factors. For two points belonging to trajectory m, $\boldsymbol{x}^{(l)}$ and $\boldsymbol{x}^{(l+1)}$, with l being in the set $\{1, ..., k\}$, the elementary factor relative to the input i is calculated as:

$$EE_i^m(\boldsymbol{x}^{(l)}) = \frac{y(\boldsymbol{x}^{(l+1)}) - y(\boldsymbol{x}^{(l)})}{\Delta}, \tag{12}$$

as $\boldsymbol{x}^{(l)}$ is increased by Δ in its i-th component [5]. After having obtained the r elementary effects of all the input parameters ($EE_i^m, i = 1, 2, ..., k, j = 1, 2, ..., r$), it is possible to compute the three sensitivity measures for each factor: μ_i, μ_i^* and σ_i. Since the elementary effects of the different trajectories are independent, the statistics can be obtained as for independent random samples:

$$\mu_i = \frac{1}{r} \sum_{m=1}^{r} EE_i^m \tag{13}$$

$$\mu_i^* = \frac{1}{r} \sum_{m=1}^{r} |EE_i^m| \tag{14}$$

$$\sigma_i^= \sqrt{\frac{1}{r-1} \sum_{m=1}^{r} (EE_i^m - \mu)^2} \tag{15}$$

where EE_i^m represents the elementary effect of the i-th input computed along trajectory m.

7.2 Application to the case study

The Elementary Effects method, described in Section 7.1, is applied to the model of the cruise-ship energy system proposed by Baldi, defined in Section 4, including the computation of the defined sensitivity measures. This will allow not only identify the non-influential parameters but also validate Baldi's model by confirming the correlations between inputs and outputs.

The input parameters, the uncertainties of which are identified in Section 6.3, are first ranked based on their values of μ_i^*. These statistics are calculated for the main output of interest: the value of the objective function in the optimization problem (i.e. the total cost). This ranking will, on the one hand, allow to identify the non-influential factors that are input to the model. The uncertainties of these will, therefore, be considered as irrelevant and their further characterization will have no interest for any future investigations on this system. For the impactful parameters, on the other hand, it will be possible to assess their relative importance with respect to the total cost. The μ_i^* values for other outputs, such as the installation sizes (i.e. multiplication factors) of the most interesting utilities, for all the inputs are similarly computed and compared.

As previously mentioned, the values of μ_i of all the considered input parameters are also computed to verify the sign of the correlations between them and certain outputs of interest. This is the case of the installation sizes of all the technologies of the energy system: y_{SOFC}, y_{PEMFC}, y_{HS}, y_{ES} and y_{GT}. The resulting values of $\mu_{i,j}$, for output j, are ranked based on their absolute values, i.e. $|\mu_{i,j}|$, subsequently

focusing only on the highly ranked input parameters. Large differences between the rankings of $\mu^*_{i,j}$ and $\mu_{i,j}$, for a given output j, will first suggest that several parameters have positive and negative effects on output j and thus, that type II errors are being avoided by considering $\mu^*_{i,j}$. Most interestingly, the signs of the input-output correlations, given by the values of $\mu_{i,j}$, are assessed by comparing them to the corresponding expected results. This will serve to verify that the model represents adequately the behavior of the actual energy system.

It is also important to mention that in this application, the calculation of the elementary effects is slightly modified with respect to Morris' original computation. It is improved, as suggested by Sin and Gernaey [79], by considering the standard deviations of both the input parameters and the output values. For a given trajectory m, the elementary effect of input i relative to ouput j is calculated as indicated by (16). In this expression, the δY_i represents the difference between the value of the considered output when X_i is altered and its value when all inputs are at nominal value, while δX_i is the variation of X_i at a given step with respect to its nominal value. Both differences are also normalized by the standard deviations of the considered output and the given input parameter, represented by σ_{Y_j} and σ_{X_i} respectively. This computation is equivalent to the one previously given in (10), if it is also normalized by σ_{Y_j} and σ_{X_i}. By doing this, it is now possible to compare the EEs of inputs with disparate orders of magnitude and of different outputs.

$$EE^m_{ij} = \frac{\delta Y_j}{\delta X_i}\frac{\sigma_{X_i}}{\sigma_{Y_j}} \tag{16}$$

A descriptive summary of the numerical implementation of the EE method for the current energy system model is presented next in Section 7.2.1. Once the corresponding code has been developed and tested, it is used to carry out two different analysis.

First, only the cost-related input parameters, that appear exclusively in the objective function of the optimization problem, are included in the study, as described in Section 7.2.2. In this way, it is guaranteed that no issues are produced by infeasibilities of the MILP problem. Costing significantly less computationally, the results are used as a means to verify the accuracy of the adapted implementation of the Morris method. In addition, the correlations between the key input parameters and the outputs of interest are also analyzed.

The second and most important analysis includes all the input parameters the uncertainty of which is characterized in Section 6 and is presented in Section 7.2.3. Unlike the first study, that entails an a priori selection of input parameters, this one attempts not to make any prior exclusions of factors. The objective is to avoid, as much as possible, involving preconceived considerations on the relevance of factors that may actually be erronous. The sensisitivity measurements computation and

the assessments previously described are, thus, focused on this final setting.

7.2.1 Numerical implementation

The application of the Morris method to the model of the cruise-ship's energy system is performed with the help of MATLAB. A code is developed to carry out all the necessary computations and simulations of the model automatically, being possible to use it with any subset of input parameters. The flowchart presented in Figure 8 depicts, in a simplistic way, the steps that are followed by the code. As shown, it is divided into three main blocks: the sampling, the simulations and the sensitivity computations. The process followed in each of these is further detailed next:

1. **The sampling**:
   Once the values for r, p and Δ are defined as desired, the first step is to generate the ensemble of sampling points. For this purpose, it is first necessary to read the labels, nominal, minimum and maximum values of the input parameters from a csv file. These input data is saved into matrices. A function subsequently takes care of the generation of the different trajectories, with the appropriate properties, according to the indications given in []. Discrete uniform probabilities are produced for each input factor, based on the values of r, p, Δ and k, and within the interval [0,1]. The randomized sample points that correspond to each factor are then calculated as shown in (17), taking account the upper and lower limits of their uncertainty intervals:

   $$X_{i,t} = LL_i + u_{i,t}(UL_i - LL_i), \tag{17}$$

   where $X_{i,t}$ represents the value of factor i in the sample point t and $u_{i,t}$ is the random value taken from the discrete uniform distribution produced for factor i at step t, $\forall i \epsilon \{1, ..., k\}$ and $\forall t \epsilon \{1, ..., r(k+1)\}$; and where LL_i and UL_i are the lower and upper bounds, respectively, of factor i.

   A total of $r(k+1)$ random sample points are therefore generated and saved in a ($r(k+1)$ x k) matrix, each of them representing the input data of a model run, of one particular studied scenario.

2. **The simulation**:
   Once the values of all input factors have been defined for each scenario, the model must be run for each of these. Within a for loop, that goes from scenario 1 until scenario $n = r(k+1)$, csv files with the data of sample point t are created and saved in the appropriate folder. In each iteration, the OSMOSE model is executed, making sure it reads the corresponding input files and runs the optimization accordingly. To avoid any errors in the reading of the input

csv files, these are deleted after each iteration. The results yielded by the given model run, concerning the outputs of interest previously mentioned (y_j, t), are read by the MATLAB code and saved. The implementation of the loop is performed with a parfor (i.e. a parallel for loop) to increase the speed of the computation by almost a factor of $1/s$, with s being the number of processors of the computer where the code is being executed.

3. **Sensitivity computations**:
   The values of $\boldsymbol{X}^1, ..., \boldsymbol{X}^n$, as well as those of $y_{TotalCost}$, and the input sizes of all technologies are transmitted to a function that computes all sensitivity measures. The standard deviations of all input parameter values, and of the different outputs of interest are first calculated. For each input factor, and for each trajectory, the step in which the concerned parameter changes value with respect to the previous one is recorded, as well as the increment it suffered. This change represents the δX_i involved in the EE_{ij}^m computation described in (16). The values of the considered outputs in these two steps are also saved. The EE_{ij}^m values, for each input-output pair and at each trajectory, are subsequently computed as indicated by (16). However, to avoid having excessively high values of EE_{ij}^m, in cases where this would be produced by very low values of σ_{y_j}, a filter is included in these calculations. Only the elementary effects of the outputs with a $\sigma_{y_j} \geq 0.0001$ are computed.

   Having the values of EE_{ij}^m, $\forall i \in \{1, ..., k\}$, $\forall j \in \{$TotalCost, SOFC, PEMFC, HS, ES, GT$\}$ and $\forall m \in \{1, ..., r\}$, the values of $\mu_{i,j}^*$ and $\mu_{i,j}$ finally calculated. These sensitivity measures are finally used to order the input parameters in descending orderof importance, as previously described.

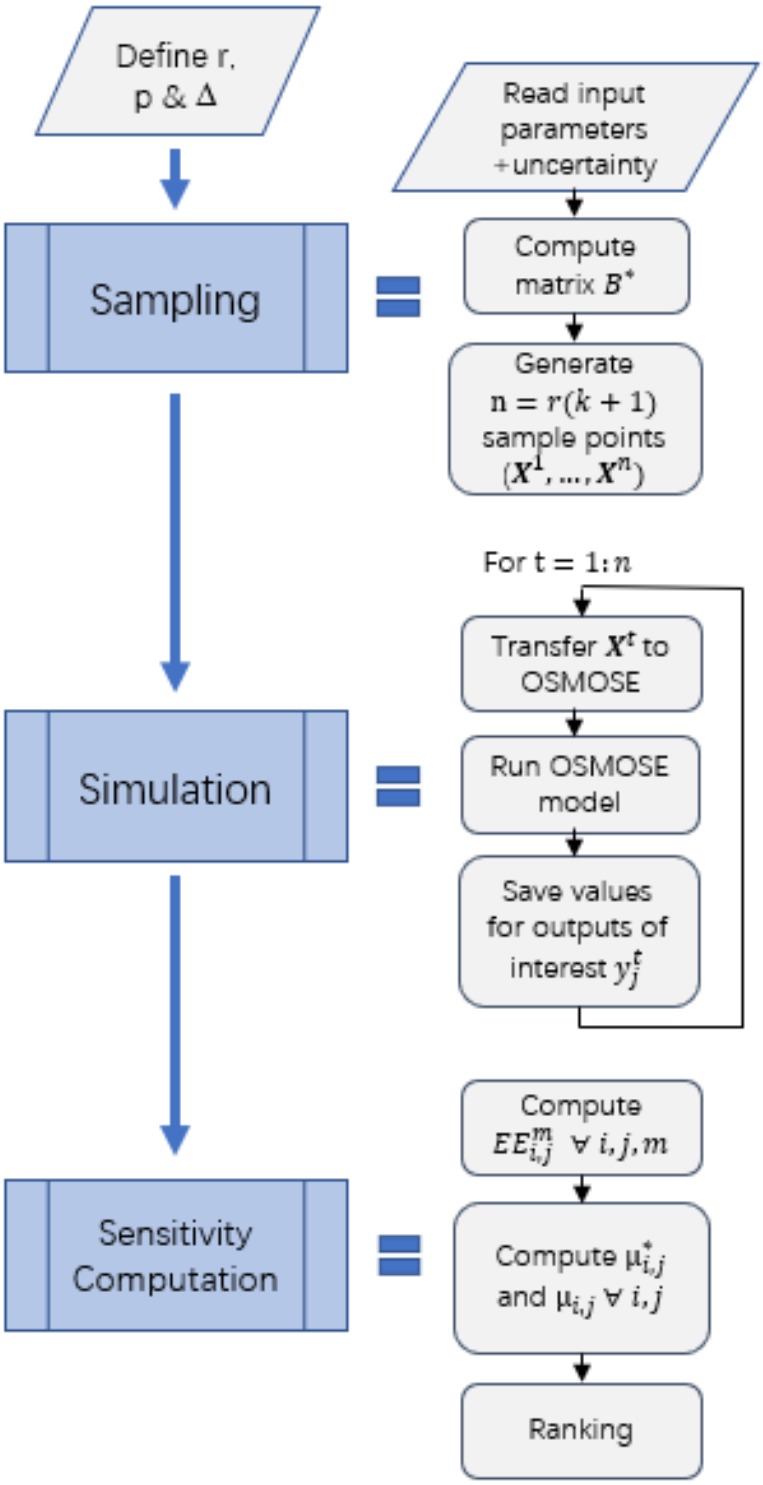

Figure 8: Flow chart of the process followed by the MATLAB code developed to implement the Morris method for the energy system's model.

7.2.2 First analysis

As previously mentioned, a simpler sensitivity analysis is initially carried out to confirm that the developed code works appropriately. It suffices, in this case, to consider a smaller subset of input parameters, which entails a significant reduction in the computational cost of the study. Since the effects of variating parameters in the objective function are rather intuitive, only the cost-related factors are input to the analysis. This simplifies the detection of errors and the verification of the results. Further, all possible issues relative to the feasibility of the optimization problems are also avoided.

The considered input values correspond to the fixed and variable investment costs of the different utilities, previously provided in Table 7. The gas price is also included in the analysis. For simplicity, each of these factors is given an uncertainty of $\pm 20\%$, except for those that have a nominal null value. The selected values for r, p and Δ are 20, 6 and 2/3, respectively. As the total number of inputs is 13, this supposes the simulation of $20(13 + 1) = 280$ scenarios.

In this analysis, the focus is made on the results of $\mu^*_{i,j}$, especially on the parameters highly ranked with respect to the total cost. In addition, plots of several input-output pairs, displaying their values across all trajectories, are generated. The corresponding linear trends are also computed and superimposed. These allow not only to observe the dispersion of the output values produced by the variation of particular factors, but also verify that the resulting trends are not counter-intuitive.

7.2.3 Final analysis

The final sensitivity analysis is the main focus of this project. As previoulsy stated, the goal is to assess the effect of having uncertainty in the input parameters of the energy system's model. The most impactful factors are to be identified, as well as the non-influential ones. As the modeler's prior considerations on the importance of the parameters can be flawed, all inputs should be included in the analysis. In this case, however, some ended up being excluded for the reasons described in Section 6. This is why a possible future work would be to finally incorporate every input parameter of the model into the sensitivity analysis.

The final set of 44 uncertain parameters, with their corresponding ranges calculated in Section 6.3 and their nominal (original) values, were included in the study. A total of r=25 trajectories were selected, producing a total number of model runs of $n = r(k+1) = 25(44+1) = 1125$. In addition, $p = 6$ and $\Delta = 2/3$ are also defined.

The indications given in Section 7.2 on the application of the Morris method to

the case study are followed in this final analysis. The corresponding results are presented in Section 7.3.2.

7.3 Results

7.3.1 First Analysis Results

The values of $\mu^*_{i,j}$ for the outputs Total Cost, y_{SOFC}, y_{PEMFC}, y_{HS} and y_{ES} are plotted in Figure 9 . The input parameters are ordered based on their impact on the total cost of the energy system and only those that satisfy $\mu^*_{i,TotalCost} \geq 0.01 \max_{i \in 1,\dots,k} \mu^*_{i,j}$ are included.

The first interesting result observed in Figure 9 is the outstandingly large value, of over 95%, of the gas price's $\mu^*_{i,TotalCost}$. This implies that the variation of this input factor produces the greatest variations on the energy system's total cost. In contrast, all the other parameters have an almost negligible effect compared to the gas price, with only the $C_{inv,var}$(ES) reaching close to a 10% of relevance.

These significant differences are not observed, however, for any of the other outputs. Although the gas price is also impactful on the utilities' installation sizes, with $\mu^*_{i,j}$ of around 0.6, so are parameters such as $C_{inv,var}(ES)$ and $C_{inv,var}(SOFC)$. In fact, $C_{inv,var}(ES)$ has values between 0.65 and 0.75 for all the technology sizes, corresponding to the highest $\mu^*_{i,j}$ value for all of them.

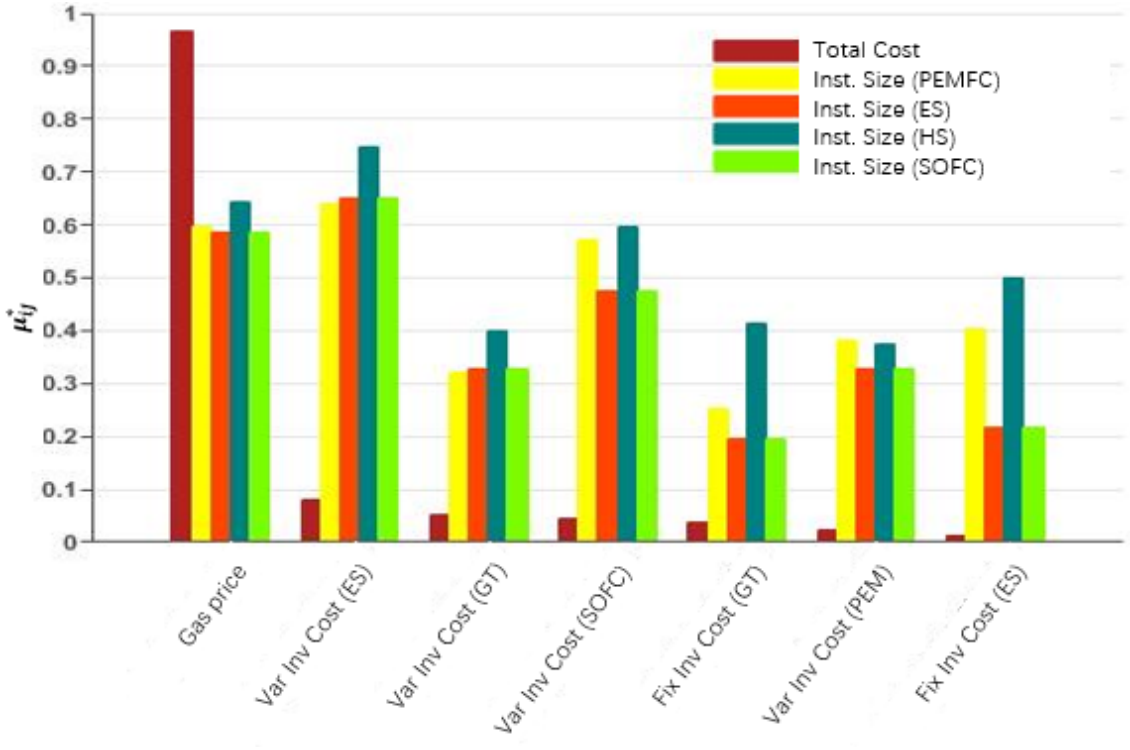

Figure 9: Values of $\mu^*_{i,j}$ for different outputs of interest (Total Cost, y_{SOFC}, y_{PEMFC}, y_{HS} and y_{ES}), with the parameters being ranked with respect to the total cost. Only the factors with $\mu^*_{i,TotalCost} \geq 0.01 \max_{i \in 1,\ldots,k} \mu^*_{i,j}$.

Input-output relationship plots

The total cost values are plotted next against its two most influential parameters, the gas price and $C_{inv,var}(ES)$, in Figure 10 and Figure 11, respectively. The trends displayed by all the respective sample points are also included. These, however, should only be taken as qualitative representations of the relationships between inputs and outputs. The aim is, thus, to assess the sign of the trends and the qualitative differences in their slopes.

In Figure 10, the dominant effect of the gas price over the other parameters, with respect to the total cost, can be observed. For a given value of gas price, the values of total cost across scenarios show little dispersion (of around 5%), even though the remaining factors are being varied. This is not the case for the effect of $C_{inv,var}(ES)$, depicted in Figure 11. The dispersion in total cost values can instead be of more than 15%, for a fixed value of $C_{inv,var}(ES)$. This plot's trend is almost unperceivable if compared to that of the total cost vs. gas price, which explains the large discrepancies in their corresponding $\mu^*_{i,j}$ values. According to the results, it is possible to say, however, that both input factors have a direct relationship with the total cost of the cruise-ship energy system.

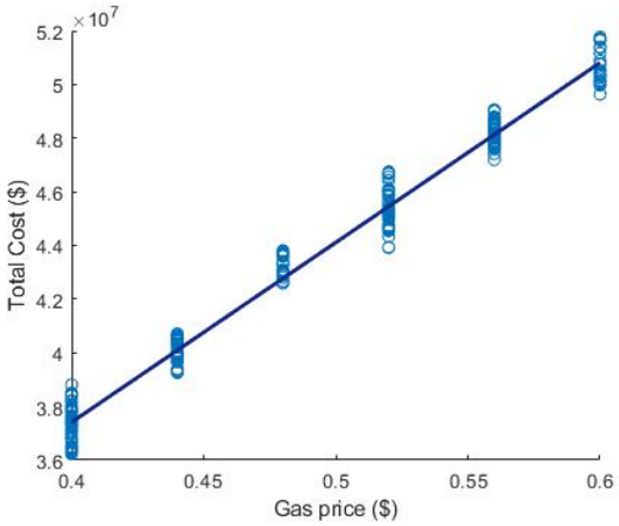

Figure 10: Plot of the total cost values against the gas price in all the scenarios simulated in the first analysis. Their linear trend is also depicted.

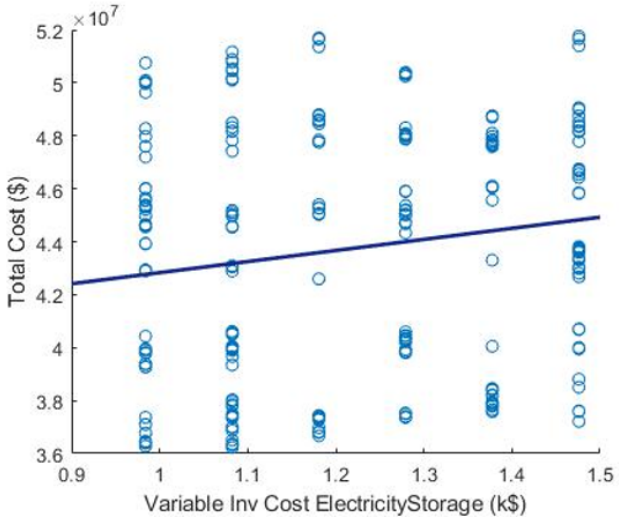

Figure 11: Plot of the total cost values against those of $C_{inv,var}$(ES) in all the scenarios simulated in the first analysis. Their linear trend is also depicted.

The impact of having uncertainty in the gas price is also assessed with respect to the installed utility sizes. Two particular cases can be observed in Figures 12 and 13, where all values of y_{SOFC} and y_{HS} are displayed, respectively, relative to this input parameter.

By comparing both figures, it can be observed that the ranges of variation of y_{HS} and y_{SOFC} are rather different. It appears that the optimal size of HS is considerably affected by uncertainty in general, this effect being remarked given the large

dispersion of its values. While this also occurs for the SOFC, its range does not exceed 5% of its average value. Despite its reduced variation, there does exist a slight positive trend between y_{SOFC} and the gas price. The opposite case applies for y_{HS}, which displays an indirect dependence on the gas price.

Although their graphs are not included in this report, it is also observed that y_{ES} presents a positive trend with respect to the fuel price, just as y_{SOFC}. In fact, the behaviors of these two outputs are very similar fir all input parameters. This behavior pairing occurs as well between y_{HS} and y_{PEMFC}.

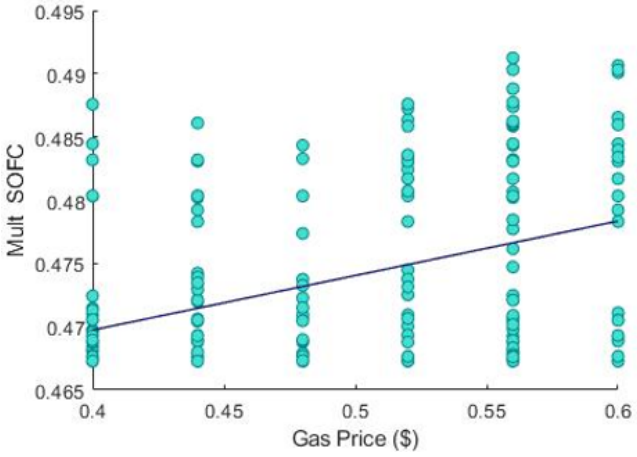

Figure 12: Plot of y_{SOFC} against the gas price in all the scenarios simulated in the first analysis. Their linear trend is also depicted.

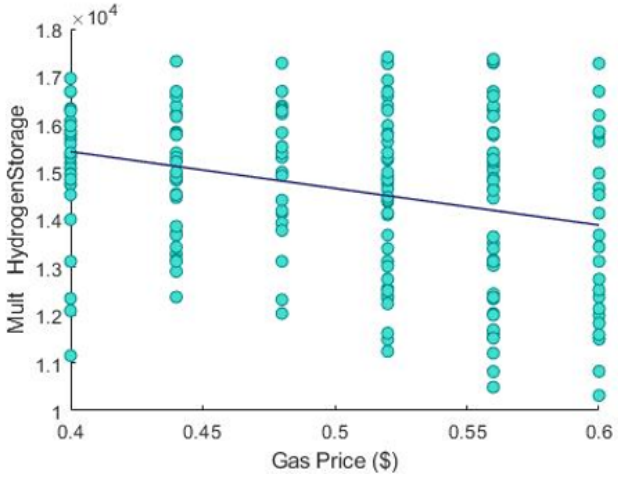

Figure 13: Plot of y_{HS} against the gas price in all the scenarios simulated in the first analysis. Their linear trend is also depicted.

The influence of the most impactful parameter in this first analysis, $C_{inv,var}(ES)$, with respect to the utilities' multiplication factors, is depicted next. y_{ES} is firstly plotted against this factor in Figure 14. In spite of being noticeably affected by other parameters' values, a dependence of y_{ES} on $C_{inv,var}(ES)$ is observed. The more the variable investment cost of this technology is increased, the smaller its optimal installed size results.

A very similar behavior is observed for the output y_{SOFC} in relation to $C_{inv,var}(ES)$, as illustrated by Figure 15. An increase in the variable cost of the batteries produces a decrease of the optimal size of the SOFC. However, in this case the change in y_{SOFC} is fairly reduced compared to that of the ES, as its range of variation remains again around 5% of its nominal value.

Finally, as observed in Figure 16, the effect on y_{PEMFC} of the presence of uncertainty in $C_{inv,var}(ES)$ is once again opposite to the previous two utility sizes. The installation of the PEMFC is, this time, favored by any increase in the value of this input parameter. In addition, the variation on the values of y_{PEMFC} is larger than those of y_{ES} and y_{SOFC}, for any given value of $C_{inv,var}(ES)$.

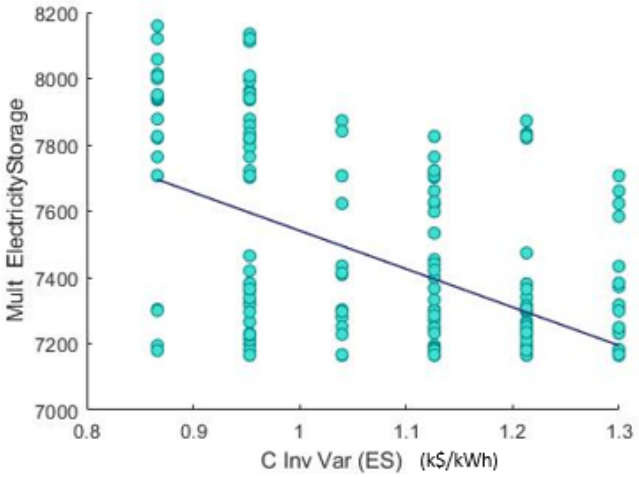

Figure 14: Plot of y_{ES} against $C_{inv,var}(ES)$ in all the scenarios simulated in the first analysis. Their linear trend is also depicted.

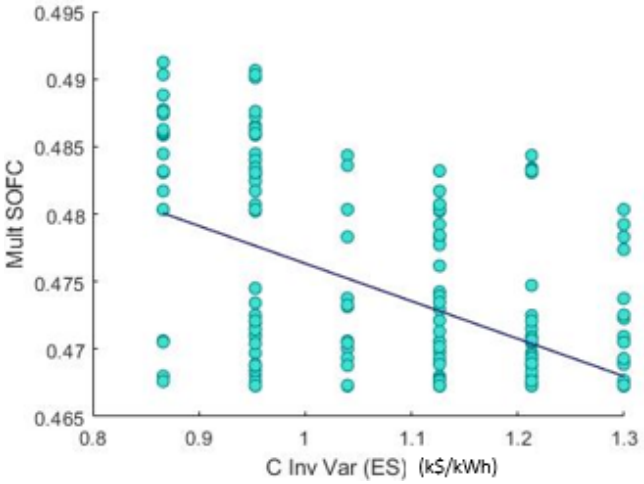

Figure 15: Plot of y_{SOFC} against $C_{inv,var}(ES)$ in all the scenarios simulated in the first analysis. Their linear trend is also depicted.

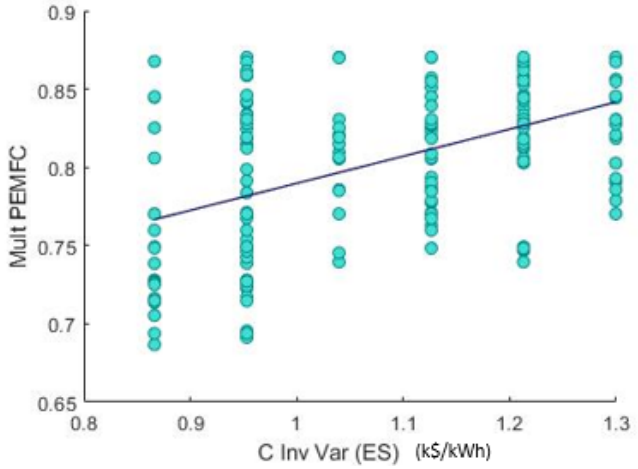

Figure 16: Plot of y_{PEMFC} against $C_{inv,var}(ES)$ in all the scenarios simulated in the first analysis. Their linear trend is also depicted.

7.3.2 Final Analysis Results

All the parameters, given their resulting values of μ^*, are ranked with respect to their impact on the total cost, as illustrated in Figure 17. It results that 36 parameters have an influence of at least 1% of the maximum value of $\mu^*_{i,TotCost}$, and only 10 an impact above 5% of the maximum, which arethe ones included in Figure 17.

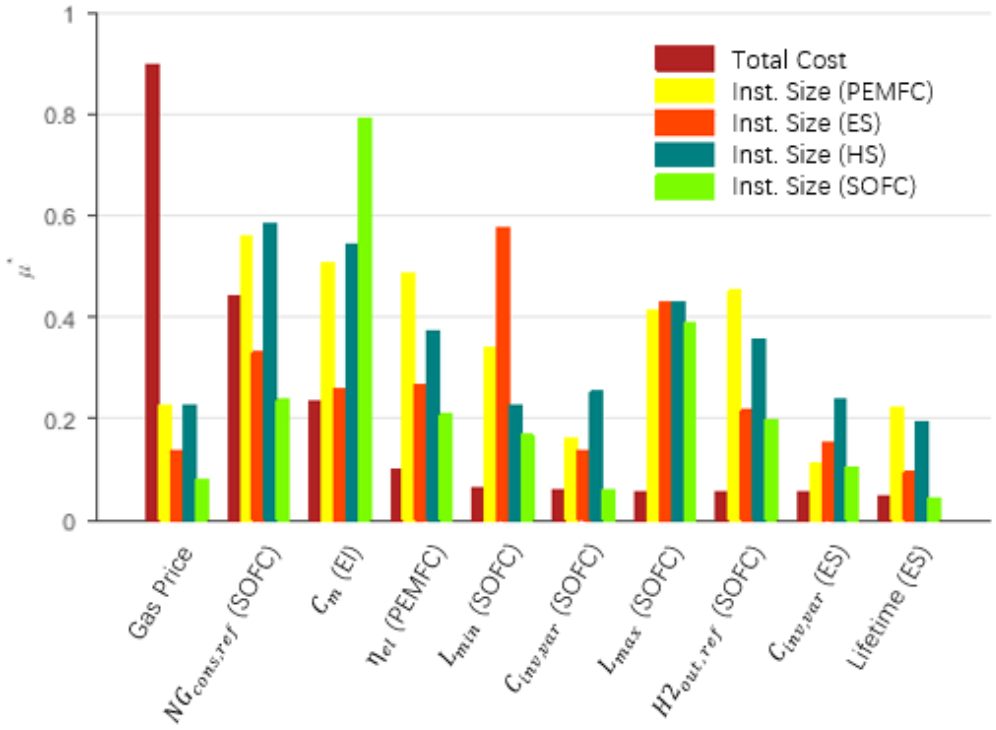

Figure 17: Values of μ^* for all the outputs of interest, with the input parameters ranked with respect to the total cost. Only the parameters that satisfy $\mu^*_{i,TotCost} \geq 0.05 \cdot max(\mu^*_{i,TotCost})$ are shown.

As observed in Figure 17, the impacts that these selected parameters have on the outputs of interest are significantly different. The input factor that has the greatest influence on the total cost is the gas price, having a value of $\mu^*_{i,TotCost}$ twice as large as the following parameter in the ranking. However, this price is not as significant for neither of the considered installed utility sizes. In addition, the values of $\mu^*_{i,TotCost}$ go under 0.1 after a few parameters, while those of all the technology sizes have a larger variety of parameters with a considerable effect on them.

The reference fuel consumption of the SOFC ($NG_{cons,ref}$ (SOFC)), related to the overall efficiency of this technology, and C_m (El) are the other factors that appear to have an important effect on the total cost. It is also interesting to see that the electrical efficiency of the PEMFC is the fourth parameter in this ranking. The following parameters are SOFC-related, for the most part, and only two factors relative to utility costs result to be impactful.

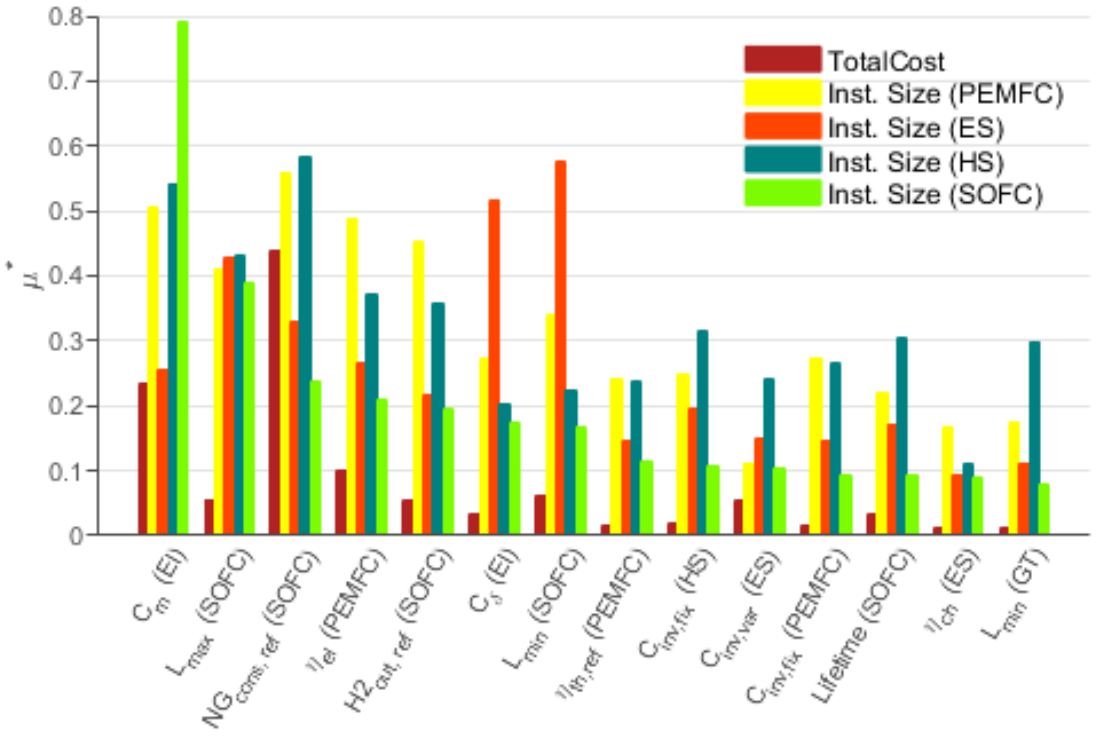

Figure 18: Values of μ^* for all the outputs of interest, with the input parameters ranked with respect to the installed size of the SOFC. Only the parameters that satisfy $\mu^*_{i,SOFC} \geq 0.1 \cdot max(\mu^*_{i,SOFC})$ are shown.

If the input parameters are ranked, instead of by their effect on the total cost, by their relevance for the SOFC's installed size, a significantly different list of results is obtained, as shown in Figure 18. Moreover, the threshold has to be set higher (to 10% of the maximum $\mu^*_{i,SOFC}$) to obtain a more effective screening. In this case, the most impactful factor is the coefficient of mean electricity demand, followed by L_{max} (SOFC), again half as large as the first. Similarly to the total cost, the efficiency-related parameters of the SOFC and the PEMFC also have an important impact, however, the factor C_δ (El) appears as influential much sooner than in the previous case.

It is noticed that a few cost-related parameters have a non-negligible influence on y_{SOFC}. However, none of them are relative to the SOFC. This implies that the utility remains optimal within the considered uncertainty range for its investment costs.

In both Figures 17 and 18, it can be observed that the sizes of the battery and of the SOFC have mainly two parameters that influence them greatly, while those of the hydrogen storage and the PEMFC are affected more evenly by the different input factors. For most parameters, these latter outputs behave in a fairly simi-

lar way. On the other hand, it can be seen that the two means of energy storage have quite contrasting impacts, just as for the case of the parameters C_δ(El) and L_{min}(SOFC).

Correlations analysis: $\mu_{i,j}$ values

Some of the values for the senstivity measure $\mu_{i,j}$, described in Section 7.1, are presented here to gain more insight and verify the sort of relationship input factors have with the utility installation sizes. This analysis remains, however, of a qualitative kind.

In Figure 19, the parameters have been ranked with respect to the absolute magnitude of $\mu_{i,SOFC}$. Only the parameters having an impact above 10% of the maximum $\mu_{i,SOFC}$ are shown.

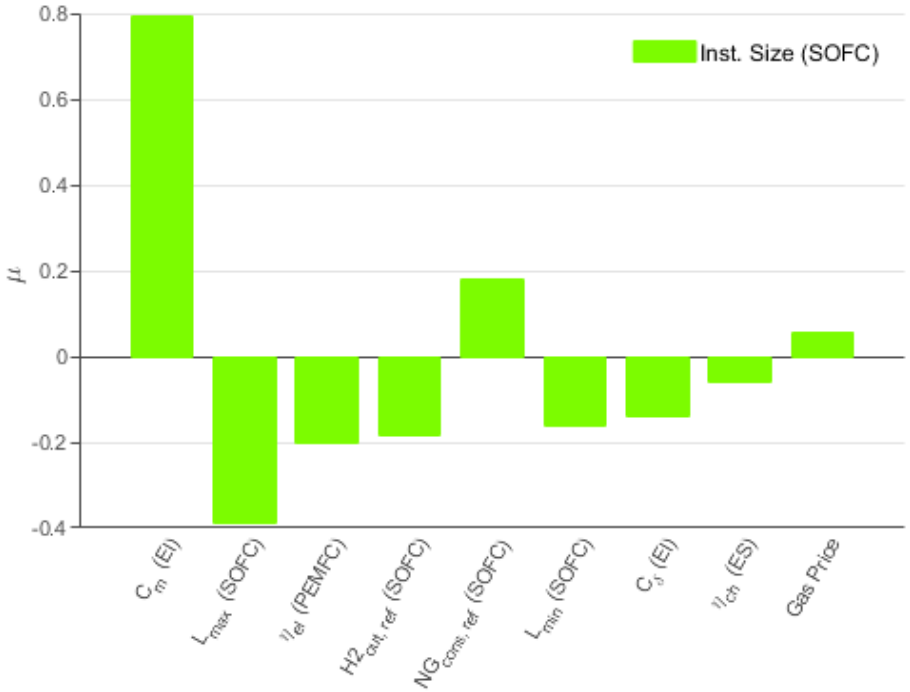

Figure 19: Values of $\mu_{i,SOFC}$, with the input parameters ranked with respect to $|mu_{i,SOFC}|$. Only parameters that are above the threshold of 10% of the maximum value of $\mu_{i,SOFC}$ are included.

Similarly to what was observed in Figure 18, the two most influential parameters on the optimal size of this technology result to be C_m (El) and L_{max}(SOFC), with the former being considerably more important. In this graph, however, it can also be seen that these two factors have opposite effects on this output. In fact, the

majority of impactful parameters present an indirect relationship with y_{SOFC}, such as η_{el}(PEMFC), $H2_{out,ref}(SOFC)$ and $L_{min}(SOFC)$. Besides C_m, only the reference amount of fuel consumed by the SOFC is positively correlated with its optimal size. As will be discussed in Section 7.4, this is related to the fact that the overall efficiency of the SOFC also affects the production of H_2 which limits the use of the PEMFC.

Figure 20 shows next the values of $\mu_{i,PEMFC}$ ranked based on their absolute value. This time only parameters with a value above 20% of the maximum absolute $\mu_{i,PEMFC}$ are considered. It is observed that the most influential factor is $NG_{cons,ref}$ (SOFC), having an opposite relationship with the PEMFC size. On the other hand, parameters such as η_{el} (PEMFC), C_m(El) or the $H2_{out,ref}$(SOFC) have a significant direct influence on the size of this technology. This is not the case, for example, of L_{min}, $Lifetime$(ES) or $C_{inv,fix}$(PEMFC). An increase in these parameters' values would most likely entail a reduction in the optimal size of the PEMFC.

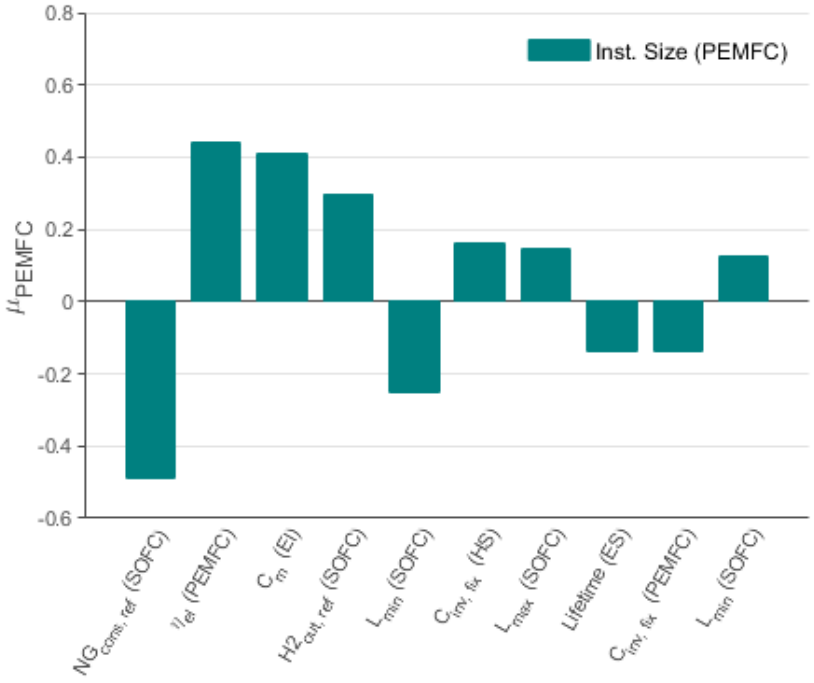

Figure 20: Values of $\mu_{i,PEMFC}$, with the input parameters ranked with respect to $|mu_{i,PEMFC}|$. Only parameters that are above the threshold of 20% the maximum value of $\mu_{i,PEMFC}$ are included.

The highest values of $\mu_{i,ES}$ have also been plotted in Figure 21, showing only the parameters with a mu_i of at least 10% of the maximum one. In this case, it is observed that both the L_{min}(SOFC) and C_δ(El) are the factors with the largest positive impact on the installed size of the battery. In contrast, L_{max}, η_{el} (PEMFC)

and C_m(El) appear to have the opposite effect on this output. In this case, it is also confirmed that the variable investment cost of this technology has a negative influence on its optimal size, although not as significant as L_{max}(SOFC), for example.

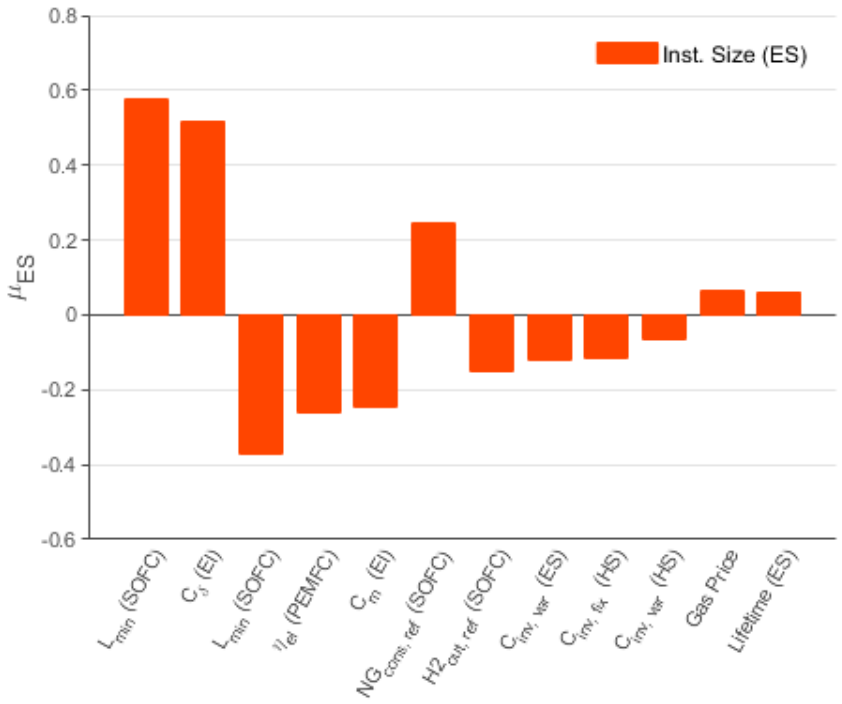

Figure 21: Values of $\mu_{i,ES}$, with the input parameters ranked with respect to $|\mu_{i,ES}|$. Only parameters that are above the threshold of 10% of the maximum value of $\mu_{i,ES}$ of are included.

Finally, a ranking of the input parameters with respect to the absolute values of $\mu_{i,GT}$ was also performed and plotted in Figure 22, allowing to study their relationship with the size of the gas turbine. As observed, only two factors have a significant and distinguishable impact on the multiplication factor of the gas turbine. Such is the case of the maximum load of the gas turbine, presenting a negative effect on this output. In simple terms, the more the capacity of the utility can be exploited, the smaller the installation can be. The second impactful parameter is the coefficient of variation of the electrical power demand, which has an influence similar in value, yet directly-related.

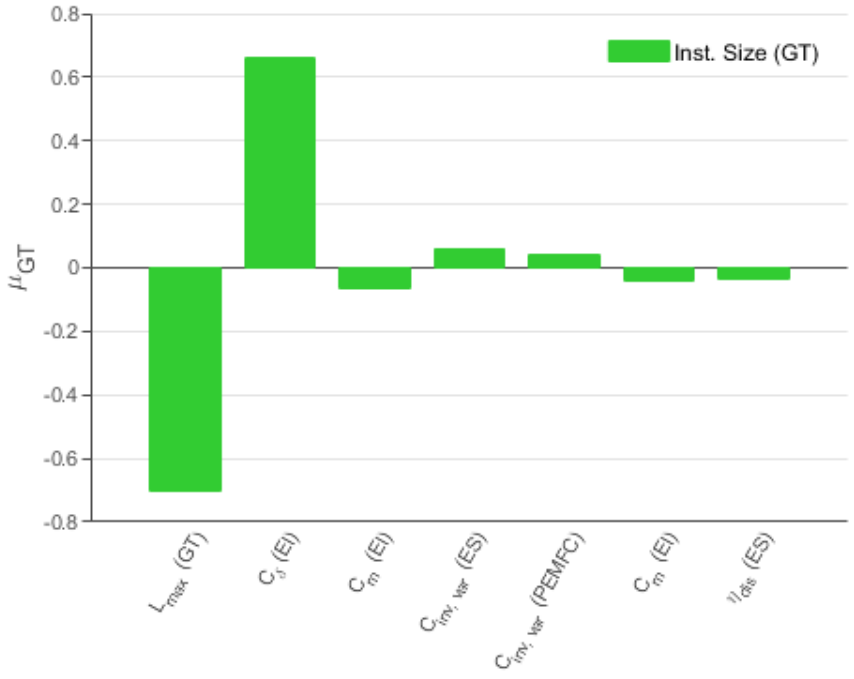

Figure 22: Values of $\mu_{i,GT}$, with the input parameters ranked with respect to $|\mu_{i,GT}|$. Only parameters that are above the threshold of 5% of the maximum value of $\mu_{i,GT}$ are included.

7.4 Analysis and discussion of the results

First analysis

The results obtained in the first analysis show the great influence of the natural gas price, over all the outputs of interest and especially the total cost. In the proposed energy system, natural gas is the only considered fuel. It is the only energy source available for satisfying all the energy demands of the cruise-ship. No matter its price, there is no cheaper alternative. Thus, natural gas must always be consumed, affecting directly the total annual cost of the energy system whenever its price changes.

The optimal installed sizes of the different technologies are also highly impacted by the variations in the gas price. This is both observed in the corresponding values of $\mu_{C_{op,NG},j}$ and the input-output scatter plots. In general terms, high fuel prices favor highly efficient, yet costly technologies. However, if the price is lowered, utilities that are less efficient, but at the same time less capital-intensive, become more and more optimal. In the end, the MILP problem is permanently optimizing the tradeoff between the investment costs and the operating costs of the designed system. This

is why the more the fuel price is increased, the larger the installed size of the SOFC becomes and the smaller the PEMFC (or HS) get.

The effect of optimizing this tradeoff is also observed when the values of other input parameters are made vary. Such is the example of the impact of variating the variable investment cost of the batteries. In this case, an increase in this technology's cost, entails a reduction in its own size, which is an intuitive result. The batteries, while being the most efficient way of storing energy, they are also more pricey. If, on top of that, its cost rises, then the combination of PEMFC plus hydrogen storage becomes more and more eligible. As a result, the larger PEMFC takes over some of the power generation of the SOFC, reducing the optimal size of the latter technology.

Based on these results, it is possible to say that the numerical implementation of the sensitivity analysis was succesful. The ranking of the input parameters but, above all, the correlations between inputs and outputs follow prior intuitions and can be easily explained.

Final analysis

The results on the final analysis show that the performed screening allows to reduce the dimension of the problem by a factor of 4. Only 10 parameters, out of the initial 44, have an influence larger than 5% of the maximum, meaning that all the remaining ones have slight or completely negligible relevance. If this work were to be followed by a robust optimization, for example, the complexity of the problem would be highly reduced. Only the uncertainty of a small subset of input parameters would need to be better characterized.

The application of the EEs method reveals that most of the parameters that are top-ranked with respect to the total cost are associated with the SOFC. This indicates that the uncertainty relative to this technology is more impactful than that of any other component, in terms of costs. Still, the fuel price stays as the most influential factor, again for the natural gas being the only energy source of the whole cruise-ship.

In all the studied scenarios of uncertainty, the SOFC remains as the main converter of energy, differing only slightly from the nominal case. Even under more unfavorable specifications, no other technology takes over the dominance of the SOFC. This is, in great measure, caused by the fact that the only real alternative technology, the gas turbine, has a very disadvantageous efficiency-cost ratio. As a consequence, the SOFC always results to be the optimal base-load solution, while the other technologies contribute more marginally. However, as it is also the most expensive utility, a decrease in the SOFC's performance does produce some changes in the optimal

system design. This is why various of its relative parameters have a considerable effect on the total cost.

The mean electrical power demand also results to be highly ranked for the total cost. With respect to this output, the mean demand appears to be significantly more relevant than its degree of fluctuation. However, this relationship does not hold for other outputs of interest, such as the sizes of the gas turbine or the batteries. This difference proves that the output on which the Morris method is based affects greatly the parameters that end up being considered as influential.

In addition, when the ranking is based on the SOFC's investment decision, the screening becomes less effective. In this case, a larger and more varied set of parameters appear to have some effect on this output. However, as many of them are shared with the cost-based ranking, it is suggested that the size of the SOFC is considerably linked with the total cost. In this ranking, the PEMFC-relative specifications also result to have a larger importance than any other utility. In fact, the effect of the GT's parameters is rather marginal. This is because the use of the this technology only becomes optimal (above the fuel cells) in periods of peak demand, which are unfrequent. Thus, it does not compete with the SOFC in the ordinary periods. This independence between the two utilities can also be observed in the results of μ_{GT}. No other parameter, besides the C_δ and its own maximum load, has a notable effect on the size of the gas turbine.

The analysis on the different μ_i values, on the other hand, also reveals interesting results on the studied energy system. Such is the case of the impact of the reference fuel consumption of the SOFC on the size of this technology. Even if the overall efficiency of the SOFC is reduced within its uncertainty range, its size is increased, meaning that its role is not largely substituted by an alternative technology. Although the PEMFC may appear as one, it is dependent on the SOFC, on its hydrogen production. Thus, even if it is done to maintain the production of H_2 and feed the PEMFC, the size of the SOFC needs to be increased. The incorporation of HS does help, however, to disconnect the operation of the two fuel cells.

Further, it is worth highlighting the fact that the most positively impactful parameter on the battery's size is the minimum load of the SOFC, rather than the limitation on the load change of this fuel cell. In fact, the latter parameter does not even appear in any of the exhibited rankings of this report. This reveals that the battery is not only working during fast transients but also in periods with low power demand.

Lastly, the fact that the parameters related to the heating part system don't have, not even the mean heat demand, significant effects on the outputs of interest should

be remarked. In addition, the investment costs of the technologies not result to be as influential as other factors. In general, efficiencies or load limitations appear in more highly ranked positions than the costs. In fact, only the variable investment cost of the battery passes the screening based on the total cost.

Chapter 5: Conclusions and Possible Future Work

8 Conclusions and Future Work

In this project, the uncertainty involved in the optimization model of a cruise-ship energy system, which was based on the use of SOFCs, was first characterized. After an initial screening and grouping of the input parameters, these were assigned with uniform distributions of uncertainty, based on a varied set of criteria. These distributions were primarily based on the spectrum of the corresponding values registered in the literature, historical or current, and in forecasts. However, an important scarcity of relevant sources was found, limiting the definition of these ranges. Time and resource limitations also interfered with this part of the work.

It was still possible, nevertheless, to recognize that the uncertainties involved in several parameters are considerable. This is particularly true for highly variable factors, such as fuel prices, and for parameters relative to the newer, still non-established technologies, such as the fuel cells. Although there are many research studies involving fuel cells, available data regarding some of their characteristics are still reduced, in comparison to more conventional technologies. Larger scarcity of information is not, nonetheless, the only reason why parameters can show high variabilities in their value across sources, as this has also been observed for well-established technologies.

Next, a Sensitivity Analysis was performed, using the Elementary Effects method (EEs), to evaluate the importance of the different uncertainties present in the optimization model. The idea was to identify the non-influential parameters, with respect to a set of outputs, and to rank the impact of the influential ones. With this study, it was also possible to validate the accuracy of the model, by verifying that the different input-output correlations followed logic. In addition, two different analysis were carried out, to assess the effect of including only a small subset of arbitrarily selected parameters, instead of all uncertain ones. The first one only involved the cost-related parameters and the final study included all the input factors the uncertainty of which was characterized in the first part. The model outputs that were considered of interest were the objective function of the optimization problem (i.e. the total cost of the designed system) and the optimal installed sizes of the main technologies (SOFC, PEMFC, HS, ES, GT).

In the main sensitivity analysis, the screening of uncertain parameters resulted to be reasonably effective when their influence was ranked with respect to the total cost. This made possible to reduce the dimension of the problem from 44 to a total of 10 parameters, all the others having an impact lower than 5% of the equivalent maximum value. Only a few parameters appeared to have a substantial effect on the total cost, with that of the gas price being the largest and the mean electricity demand the the second. It was also noticed that the optimal sizes of the different

technologies were greatly affected by multiple factors. Most of these corresponded to the average power demand, its deviation from the mean, or SOFC-related parameters. In addition, unlike what is often expected or assumed, the cost parameters of the technologies did not result to be the most influential ones for any of the outputs, not even the total cost. The factors relative to the heat demand, on the other hand, were also shown to be non-influential, as they virtually do not appear in any of the rankings.

The analysis of correlations yielded rather reasonable results. It allowed not only to identify more clearly the most influential parameters for each technology size, but also to confirm the type of relationship they have with these inputs. It helped to understand better the role that these utilities have in the proposed energy system. For instance, the impactful parameters on the battery size made it clear that it does not work only during fast transients, but also during periods of low electricity demand. The gas turbine, on the other hand, is essentially only affected by the variation of power demand, implying that it only operates after drastic increases of demand.

Finally, an answer should be given to the question on if the incorporation of uncertainty affects the optimality of the SOFC in this energy system. In this case, not really. This does not mean, however, that accounting for uncertainty has therefore no impact on optimal system design. The question here is that, as the only real alternative technology to the SOFC is the gas turbine, it would only stop being optimal if the properties of the GT surpassed those of the SOFC. Since the efficiency of the GT is assumed to be very low, and at a rather high cost, this technology always remains suboptimal in the present system. However, if other alternative utilities, with more favorable characteristics were considered in the energy system, the present uncertainties could make the SOFC suboptimal in some scenarios.

With respect to the future work, it would be interesting to finally incorporate absolutely all input parameters to the study. In other words, the factors that were excluded for the mentioned limitations, should be ultimately included, to obtain complete final results on the presence and effect of uncertainty. As proven earlier, arbitrarily omitted parameters can actually end up being the most influential ones. Moreover, the EEs-based sensitivity analysis can be followed by the application of a second SA method, such as variance-based methods, to perform a global sensitivity study. This would guarantee that the results are not, to any extent, dependent on the sample points and that all interactions between the different input uncertainties are accounted for. Finally, the impact of uncertainty could also be assessed by Robust Optimization. In this case, the parameter uncertainty would be incorporated into the optimization problem, in both the objective function and the constraints. This would allow to evaluate the direct impact of considering uncertainty in the

optimization on the optimal energy system design. The corresponding results could then be compared to those of the sensitivity analysis, as their evaluation of the relevance of uncertainty could be considerably different.

References

[1] W. L. Becker, R. J. Braun, M. Penev, and M. Melaina. Design and technoeconomic performance analysis of a 1mw solid oxide fuel cell polygeneration system for combined production of heat, hydrogen, and power. *Journal of Power Sources*, 200:34–44, February 2012.

[2] Alexandros Arsalis and Mads P. Nielsen. Modeling and off-design performance of a 1kwe HT-PEMFC (high temperature-proton exchange membrane fuel cell)-based residential micro-CHP (combined-heat-and-power) system for Danish single-family households. *Energy*, 36(2):993–1002, 2011.

[3] Francesco Baldi, Ligang Wang, and Francois Marechal. Integration of solid oxide fuel cells in cruise ship energy systems.

[4] Singhal, Subhash C. Solid Oxide Fuel Cells. *Interface, The Electrochemical Society*, 2007.

[5] Saltelli, Andrea, Ratto, Marco, Andres, Terry, Campolongo, Francesca, Cariboni, Jessica, Gatelli, Debora, Saisana, Michaela, and Tarantola, Stefano. *Global Sensitivity Analysis. The Primer*. Wiley edition, January 2008.

[6] Francesco Baldi. *Modelling, analysis and optimization of ship energy systems.* PhD thesis, Chalmers University of Technology, 2016.

[7] About the Cruise Ship Industry | http://www.cruiseshipjobsnetwork.com/cruise/cruise-ship-industry/.

[8] Cruise Industry Overview. Technical report, Florida-Caribbean Cruise Association, Florida, 2017.

[9] Miola, A., B. Ciuffo, Giovine, E., and Marra, M. Regulating air emissions from ships. The state of the art on methodologies, technologies and policy options. Technical report, Joint Research Centre Reference Report, Luxembourg, 2010.

[10] S. Brynolf, M. Magnusson, E. Fridell, and K. Andersson. Compliance possibilities for the future ECA regulations through the use of abatement technologies or change of fuels. *Transportation Research Part D: Transport and Environment*, 28:6–18, May 2014.

[11] Rami El Geneidy, Kevin Otto, Pekka Ahtila, Pentti Kujala, Kari Sillanpaa, and Tero Maki-Jouppila. Increasing energy efficiency in passenger ships by novel energy conservation measures. *Journal of Marine Engineering & Technology*, 17(2):85–98, May 2018.

[12] Dimopoulos, G. G., Kougioufas, A. V., and Frangopoulos, C. A. Synthesis, design and operation optimization of a marine energy system. *Energy*, 33(2):180–188, February 2008.

[13] Stambouli, A. B. and Traversa, E. Fuel cells, an alternative to standard sources of energy. *Renewable and Sustainable Energy Reviews*, 6(3):295–304, 2002.

[14] L. van Biert, M. Godjevac, K. Visser, and P. V. Aravind. A review of fuel cell systems for maritime applications. *Journal of Power Sources*, 327:345–364, September 2016.

[15] Stefano Moret. *Strategic energy planning under uncertainty*. PhD thesis, Ecole Polytechnique Federale de Lausanne, Lausanne, Switzerland, October 2017.

[16] Georgios Mavromatidis, Kristina Orehounig, and Jan Carmeliet. Uncertainty and global sensitivity analysis for the optimal design of distributed energy systems. *Applied Energy*, 214:219–238, March 2018.

[17] Global merchant fleet - number of ships by type 2017 | Statistic | https://www.statista.com/statistics/264024/number-of-merchant-ships-worldwide-by-type/.

[18] Cruise Industry Statistics | http://www.repositioncruises.com/cruise-industry/.

[19] Marty, P., Hetet, J.-F., Chalet, D., and Corrignan, P. Exergy Analysis of Complex Ship Energy Systems. *Exergy*, 18:127, April 2016.

[20] Francesco Baldi, Fredrik Ahlgren, Tuong-Van Nguyen, Cecilia Gabrielii, and Karin Andersson. Energy and exergy analysis of a cruise ship. In *DIVA*. Pau University, 2015.

[21] Cruise ship Emissions | http://tourismdashboard.org/explore-the-data/cruise-ship/.

[22] Sam Morgan. Daily emissions of cruise ships same as one million cars, July 2017.

[23] Evert A. Bouman, Elizabeth Lindstad, Agathe I. Rialland, and Anders H. StrÃ¸mman. State-of-the-art technologies, measures, and potential for reducing GHG emissions from shipping, A review. *Transportation Research Part D: Transport and Environment*, 52:408–421, May 2017.

[24] A. Armellini, S. Daniotti, P. Pinamonti, and M. Reini. Evaluation of gas turbines as alternative energy production systems for a large cruise ship to meet new maritime regulations. *Applied Energy*, 211:306–317, February 2018.

[25] Maria E. Mondejar, Fredrik Ahlgren, Marcus Thern, and Magnus Genrup. Quasi-steady state simulation of an organic Rankine cycle for waste heat recovery in a passenger vessel. *Applied Energy*, 185:1324–1335, January 2017.

[26] Baldi, F., Ahlgren, F., Melino, F., Gabrielli, C., and Andersson, K. Optimal load allocation of complex ship power plants,. *Energy Conversion and Management*, 124:344–356, September 2016.

[27] Massardo, A. and Lubelli, F. Internal reforming solid oxide fuel cell-gas turbine combined cycles (IRSOFC-GT): part ACell model and cycle thermodynamic analysis. 1998.

[28] Ana Carolina Riekstin, Sean James, Aman Kansal, Jie Liu, and Eric Peterson. No More Electrical Infrastructure: Towards Fuel Cell Powered Data Centers. *SIGOPS Oper. Syst. Rev.*, 48(1):39–43, May 2014.

[29] V. W. Adams. Possible fuel cell applications for ships and submarines. *Journal of Power Sources*, 29(1):181–192, January 1990.

[30] Gunter Sattler. Fuel cells going on-board. *Journal of Power Sources*, 86(1):61–67, March 2000.

[31] William H. Kumm and Jr Homer L., Lisie. Feasibility Study Of Repowering the USCGC VINDICATOR (WMEC-3) With Modular Diesel Fueled Direct Fuel Cells. page 202, May 1997.

[32] Hamburg, Messe. Fuel cells in maritime operation - low emissions in port and at sea - Renewable Energy Focus.

[33] Anonymous. Foss Joins Sandia on Hydrogen Fuel Cells for Ships. *Refinery Tracker; Houston*, 6(6):10–11, 2014.

[34] Royal Caribbean to Test Fuel Cell on High-End Newbuild | https://www.maritime-executive.com/article/royal-caribbean-to-test-fuel-cell-on-high-end-newbuild.

[35] Keno Leites, Ansgar Bauschulte, Michael Dragon, Stefan Krummrich, and Pedro Nehter. SchIBZ - Design Of Different Diesel Based Fuel Cell Systems for Seagoing Vessels and Their Evaluation. *ECS Transactions*, 42(1):49–58, April 2012.

[36] Solid oxide fuel cell, July 2018. Page Version ID: 852112980.

[37] Laosiripojana, Navadol, Wiyaratn, Wisitsree, Kiatkittipong, Worapon, Arpornwichanop, Arnornchai, Soottitantawat, Apinan, and Assabumrungrat, Suttichai. Reviews on Solid Oixde Fuel Cell Technology. *Enginnering Journal*, 13(1), January 2009.

[38] Badwal, S. P. S., Giddey, S., Munnings, C., and Kulkarni, A. Review of Progress in High Temperature Solid Oxide Fuel Cells. *Journal of the Australian Ceramics Society*, 50(1):23–37, 2014.

[39] Comprehensive review of methane conversion in solid oxide fuel cells: Prospects for efficient electricity generation from natural gas. *Progress in Energy and Combustion Science*, 54:1–64, May 2016.

[40] Why SOFC Technology? | Department of Energy | https://www.energy.gov/fe/why-sofc-technology.

[41] Buonomano, A., Calise, F., d'Accadia, M. D., Palombo, A., and Vicidomini, M. Hybrid solid oxide fuel cells-gas turbine systems for combined heat and power: A review. *Applied Energy*, 156:32–85, October 2015.

[42] SOLIDpower expands production capacity, SOFC runtime record. *Fuel Cells Bulletin*, 2017(12):9, December 2017.

[43] Tu, H. and Stimming, U. Advances, aging mechanisms and lifetime in solid-oxide fuel cells. *Journal of Power Sources*, 127(1):284–293, March 2004.

[44] Proton-exchange membrane fuel cell, August 2018. Page Version ID: 853345500.

[45] Ling Jun Tan, Chen Yang, and Nana Zhou. Performance of the Solid Oxide Fuel Cell (SOFC)/Proton-Exchange Membrane Fuel Cell (PEMFC) Hybrid System. *Chemical Engineering & Technology*, 39(4):689–698, April 2016.

[46] Andrew L. Dicks, R. G. Fellows, C. Martin Mescal, and Clive Seymour. A study of SOFC-PEM hybrid systems. *Journal of Power Sources*, 86(1):501–506, March 2000.

[47] Kyeongmin Oh, Gisu Jeong, EunAe Cho, Whangi Kim, and Hyunchul Ju. A CO poisoning model for high-temperature proton exchange membrane fuel cells comprising phosphoric acid-doped polybenzimidazole membranes. *International Journal of Hydrogen Energy*, 39(36):21915–21926, December 2014.

[48] Karthik Subramanyan, Urmila M. Diwekar, and Amit Goyal. Multi-objective optimization for hybrid fuel cells power system under uncertainty. *Journal of Power Sources*, 132(1):99–112, May 2004.

[49] Karthik Subramanyan and Urmila M. Diwekar. Optimizing model complexity with application to fuel cell based power systems. *Chemical Engineering and Processing: Process Intensification*, 46(11):1116–1128, November 2007.

[50] Cogeneration of Hydrogen and Power using solid oxide based system fed by methane rich gas | www.fch.europa.eu.

[51] A Review of Urban Energy System Models: Approaches, Challenges and Opportunities. *Renewable and Sustainable Energy Reviews*, 16.6:3847–3866, August 2012.

[52] I. E. Grossmann, R. M. Apap, B. A. Calfa, P. Garcia-Herreros, and Q. Zhang. Mathematical Programming Techniques for Optimization under Uncertainty and Their Application in Process Systems Engineering. *Theoretical Foundations of Chemical Engineering*, 51(6):893–909, November 2017.

[53] Steve Pye, Nagore Sabio, and Neil Strachan. An integrated systematic analysis of uncertainties in UK energy transition pathways. *Energy Policy*, 87:673–684, December 2015.

[54] Dubuis, M. *Energy System Design under Uncertainty.* PhD thesis, EPFL, Lausanne, Switzerland, 2012.

[55] Wenjie Gang, Godfried Augenbroe, Shengwei Wang, Cheng Fan, and Fu Xiao. An uncertainty-based design optimization method for district cooling systems. *Energy*, 102:516–527, May 2016.

[56] DNV-GL guideline for large maritime battery systems. Technical Report, DNV-GL, 2014.

[57] Patrick Adametz, Christian Potzinger, Stefan Muller, Karsten Muller, Markus Preibinger, Raphael Lechner, Dieter Bruggemann, Markus Brautsch, and Wolfgang Arlt. Thermodynamic Evaluation and Carbon Footprint Analysis of the Application of Hydrogen-Based Energy-Storage Systems in Residential Buildings. *Energy Technology*, 5(3):495–509, March 2017.

[58] Fazlollahi, S., Bungener, S. L., Mandel, P., Becker, G., and Marechal, F. Multi-objectives, multi-period optimization of district energy systems: I. Selection of typical operating periods. *Computers and Chemical Engineering*, 65:54–66, June 2014.

[59] Pinch analysis, February 2018. Page Version ID: 825268354.

[60] Process integration, April 2018. Page Version ID: 833608872.

[61] Francois Marechal and Boris Kalitventzeff. Process integration: Selection of the optimal utility system. *Computers & Chemical Engineering*, 22:S149–S156, March 1998.

[62] European LNG Infrastructure Project - A feasibility study for an LNG filling station infrastructure and test of recommendations. Technical Report, Danish Maritime Authority, Copenhagen, Denmark.

[63] Abdullah Al-Sharafi, Ahmet Z. Sahin, Tahir Ayar, and Bekir S. Yilbas. Techno-economic analysis and optimization of solar and wind energy systems for power generation and hydrogen production in Saudi Arabia. *Renewable and Sustainable Energy Reviews*, 69:33–49, March 2017.

[64] Richard Turton, Richard C. Bailie, Wallace B. Whiting, and Joseph A. Shaeiwitz. *Analysis, Synthesis and Design of Chemical Processes*. Pearson Education, December 2008. Google-Books-ID: kWXyhVXztZ8C.

[65] Sensitivity analysis, May 2018. Page Version ID: 842302184.

[66] Afzal S. Siddiqui and Chris Marnay. Addressing an Uncertain Future Using Scenario Analysis. August 2018.

[67] Jiyong Kim, S. Murat Sen, and Christos T. Maravelias. An optimization-based assessment framework for biomass-to-fuel conversion strategies. *Energy & Environmental Science*, 6(4):1093–1104, March 2013.

[68] Yong-Ho Kwon, Ho-Young Kwak, and Si-Doek Oh. Exergoeconomic analysis of gas turbine cogeneration systems. *Exergy, An International Journal*, 1(1):31–40, January 2001.

[69] Natural Gas Prices Forecast: Long Term 2018 to 2030 | Data and Charts - COMSTAT Data Hub.

[70] PRICE NATURAL GAS (HENRY HUB) | http://markets.businessinsider.com/commodities/natural-gas-price.

[71] E. Fontell, T. Kivisaari, N. Christiansen, J. B. Hansen, and J. Palsson. Conceptual study of a 250kw planar SOFC system for CHP application. *Journal of Power Sources*, 131(1):49–56, May 2004.

[72] Combined Heat and PowerTechnology Fact Sheet Series. Technical report, U.S. Department of Energy, July 2016.

[73] B. T. Kuhn, G. E. Pitel, and P. T. Krein. Electrical properties and equalization of lithium-ion cells in automotive applications. In *2005 IEEE Vehicle Power and Propulsion Conference*, pages 5 pp.–, September 2005.

[74] H. I. H. Saravanamuttoo, Gordon Frederick Crichton Rogers, and Henry Cohen. *Gas Turbine Theory*. Pearson Education, 2001. Google-Books-ID: ummg5F227WoC.

[75] L. Barelli, G. Bidini, F. Gallorini, and A. Ottaviano. An energetic exergetic comparison between PEMFC and SOFC-based micro-CHP systems. *International Journal of Hydrogen Energy*, 36(4):3206–3214, February 2011.

[76] F. Barbir and T. Gomez. Efficiency and economics of proton exchange membrane (PEM) fuel cells. *International Journal of Hydrogen Energy*, 22(1027-1037), 1997.

[77] Suthida Authayanun, Mohamed Mamlouk, and Amornchai Arpornwichanop. Maximizing the efficiency of a HT-PEMFC system integrated with glycerol reformer. *International Journal of Hydrogen Energy*, 37(8):6808–6817, April 2012.

[78] Jerome Morio. Global and local sensitivity analysis methods for a physical system. *European Journal of Physics*, 32(6):1577, 2011.

[79] Gurkan Sin and Krist V. Gernaey. Improving the Morris method for sensitivity analysis by scaling the elementary effects. In Jacek Jezowski and Jan Thullie, editors, *Computer Aided Chemical Engineering*, volume 26 of *19 European Symposium on Computer Aided Process Engineering*, pages 925–930. Elsevier, January 2009.